Open burning of rice, corn and wheat straws: primary emissions, photochemical aging, and secondary organic aerosol formation

Zheng Fang[1,3], Wei Deng[1,3], Yanli Zhang[1,2], Xiang Ding[1], Mingjin Tang[1], Tengyu Liu[1], Qihou Hu[1], Ming Zhu[1,3], Zhaoyi Wang[1,3], Weiqiang Yang[1,3], Zhonghui Huang[1,3], Wei Song[1,2], Xinhui Bi[1], Jianmin Chen[4], Yele Sun[5], Christian George[6], Xinming Wang[1,2,*]

[1]State Key Laboratory of Organic Geochemistry and Guangdong Key Laboratory of Environment Protection and Resources Utilization, Guangzhou Institute of Geochemistry, Chinese Academy of Sciences, Guangzhou 510640, China

[2]Center for Excellence in Regional Atmospheric Environment, Institute of Urban Environment, Chinese Academy of Sciences, Xiamen 361021, China

[3]University of Chinese Academy of Sciences, Beijing 100049, China

[4]Shanghai Key Laboratory of Atmospheric Particle Pollution and Prevention, Department of Environmental Science & Engineering, Fudan University, Shanghai 200433, China

[5]Institute of Atmospheric Physics, Chinese Academy of Sciences, Beijing 100029, China

[6]Institut de Recherches sur la Catalyse et l'Environment de Lyon (IRCELYON), CNRS, UMR5256, Villeurbanne F-69626, France

Correspondence to: X. Wang (wangxm@gig.ac.cn)

Abstract. Agricultural residues are among the most abundant biomass burned globally, especially in China. However, there is rare information on primary emissions and photochemical evolution of agricultural residues burning. In this study, indoor chamber experiments were conducted to investigate primary emissions from open burning of rice, corn and wheat straws and their photochemical aging as well. Emission factors of NO_x, NH_3, SO_2, 67 non-methane hydrocarbons (NMHCs), particulate matter (PM), organic aerosol (OA) and black carbon (BC) under ambient dilution conditions were determined. Olefins accounted for >50% of the total speciated NMHCs emission (2.47 to 5.04 g kg^{-1}), indicating high ozone formation potential of straw burning emissions. Emission factors of PM (3.73 to 6.36 g kg^{-1}) and primary organic carbon (POC, 2.05 to 4.11 gC kg^{-1}), measured at dilution ratios of 1300 to 4000, were lower than those reported in previous studies at low dilution ratios, probably due to the evaporation of semi-volatile organic compounds under high dilution conditions. After photochemical aging with OH exposure range of (1.97-4.97)×10^{10} molecule cm^{-3} s in the chamber, large amounts of secondary organic aerosol (SOA) were produced with OA mass enhancement ratios (the mass ratio of total OA to primary OA) of 2.4-7.6. The 20 known precursors could only explain 5.0-27.3% of the observed SOA mass, suggesting that the major precursors of SOA formed from open straw burning remain unidentified. Aerosol mass spectrometry (AMS) signaled that the aged OA contained less hydrocarbons but more oxygen- and nitrogen-containing compounds than primary OA, and carbon oxidation state (OS_c) calculated with AMS resolved O/C and H/C ratios increased linearly (p<0.001) with OH exposure with quite similar slopes.

1 Introduction

On the global scale, biomass burning (BB) is the main source of primary organic carbon (OC) (Bond et al., 2004; Huang et al., 2015), black carbon (BC) (Bond et al., 2013; Cheng et al., 2016), and brown carbon (BrC) (Laskin et al., 2015). It is also the second largest source of non-methane organic gases (NMOGs) in the atmosphere (Yokelson et al., 2008; Stockwell et al., 2014). In addition, atmospheric aging of biomass burning plumes produces substantial secondary pollutants. The increase of tropospheric ozone (O_3) in aged biomass burning plumes could last for days and even months (Thompson et al., 2001; Duncan et al., 2003; Real et al., 2007) with complex atmospheric chemistry (Arnold et al., 2015; Müller et al., 2016). Moreover, biomass and biofuel burning could contribute up to 70% of global secondary organic aerosols (SOA) burden (Shrivastava et al., 2015) and hence influence the seasonal variation of global SOA (Tsigaridis et al., 2014). Since it produces large amounts of primary and secondary pollutants, it is essential to characterize primary emissions and photochemical evolution of biomass burning in order to better understand its impacts on air quality (Huang et al., 2014), human health (Alves et al., 2015) and climate change (Andreae et al., 2004; Koren et al., 2004; Laskin et al., 2015; Huang et al., 2016).

Open burning of agricultural residues, a convenient and inexpensive way to prepare for the next crop planting, could induce severe regional haze events (Cheng et al., 2013; Tariq et al., 2016). Among all the biomass burning types, agricultural residues burning in the field is estimated to contribute ~10% of the total mass burned globally (Andreae and Merlet, 2001), and its relative contribution is even larger in Asia (~34%) and especially in China (>60%) (Streets et al., 2003) where >600 million people live in the countryside (NBSPRC, 2015). Agricultural residues burned in China were estimated to be up to 160 million tons in 2012, accounting for ~40% of the global agricultural residues burned (Li et al., 2016). As estimated by Tian et al. (2011), agricultural residues burning contributed to 70-80% of non-methane

hydrocarbons (NMHCs) and particulate matter (PM) emitted by biomass burning in China during 2000-2007. A better understanding of the role agricultural residual burning plays in air pollution in China and elsewhere requires better characterization of primary emission and atmospheric aging of emitted trace gases and particles for different types of agricultural residues under different burning conditions.

In the pasted two decades, there have been increasing numbers of characterization of biomass burning emissions. Andreae and Merlet (2001) summarized emission factors (EFs) for both gaseous and particulate compounds from seven types of biomass burning. Akagi et al. (2011) updated the emission data for fourteen types of biomass burning, and newly identified species were included. Since biomass types and combustion conditions may differ in different studies, reported emission factors are highly variable, especially for agricultural residues burning (Li et al., 2007; Cao et al., 2008; Zhang et al., 2008; Li et al., 2009; Yokelson et al., 2011; Brassard et al., 2014; Sanchis et al., 2014; Wang et al., 2014; Ni et al., 2015; Kim Oanh et al., 2015; Stockwell et al., 2016; Bruns et al., 2017; Li et al., 2017; Thacik et al., 2017). Moreover, previous studies on agricultural residues burning were mostly carried out near fire spots or in chambers with low dilution ratios. Since biomass burning organic aerosols (BBOA) are typically semi-volatile (Grieshop et al., 2009b; May et al., 2013), it is expected that measured BBOA emission factors would be affected by dilution processes (Lipsky et al., 2006), and BBOA emission factors under ambient dilution conditions are still unclear. Furthermore, knowledge in NMOGs emitted from agricultural residues burning is very limited. As reported by Stockwell et al. (2015), ~21% (in weight) of NMOGs in biomass burning plumes have not been identified yet. Therefore, comprehensive measurement and characterization of gaseous and particulate species emitted by agricultural residues burning under ambient dilution conditions are urgently needed.

Great attention has been drawn to SOA formation and transformation in biomass burning

plumes recently, since significant increase of mass and apparent change in physicochemical characteristics of aerosols have been observed during atmospheric aging of biomass burning plumes in both field and laboratory studies (Grieshop et al., 2009a,b; Hennigan et al., 2011; Heringa et al., 2011; Lambe et al., 2011; Jolleys et al., 2012; Giordano et al., 2013; Martin et al., 2013; Ortega et al., 2013; Ding et al., 2016a; Ding et al., 2016b; Ding et al., 2017). For agricultural residues burning, evolution processes have not been well characterized yet. To our knowledge, up to now there is only a chamber study (Li et al., 2015) which has investigated the evolution of aerosol particles emitted by wheat straw burning under dark conditions. Although field studies (Adler et al., 2011; Liu et al., 2016) witnessed the evolution in mass concentrations, size distribution, oxidation state and optical properties of aerosol particles emitted by agricultural residues burning, these changes could be also influenced by other emission sources and meteorological conditions as well. Since NMOGs emitted by agricultural residues burning are not fully quantified, it is still challenging to predict the concentration and physicochemical properties of SOA resulted from biomass burning (Spracklen et al., 2011; Jathar et al., 2014; Shrivastava et al., 2015; Hatch et al., 2017). Bruns et al. (2016) suggsted that the 22 major NMOGs identified in residential wood combustion could explain the majority of observed SOA, but it remains unclear whether identified NMOGs emitted by agricultural residues burning could fully (or at least largely) explain the SOA formed. In addition, aerosol mass spectrometry (AMS) has been widely used to characterize sources and evolution of ambient OA (Zhang et al., 2011). Although agricultural residues burning is an important type of biomass burning in Asia and especially in China, the lack of AMS spectra for primary and aged OA from agricultural residues burning significantly limits further application of AMS in BBOA research.

In this study, plumes from agricultural residues open burning were directly introduced into a large indoor chamber to firstly characterize primary emissions and then investigate their

photochemical evolution under ~25°C and ~50% relative humidity. Corn, rice and wheat straws, which accounts for more than 90% of the crop residues burned in China (FAO, 2017), were chosen. A suite of advanced online and offline techniques were utilized to measure gaseous and particulate species, enabling comprehensive measurements of emission factors of gaseous and particulate compounds for burning of each types of straw under ambient dilution conditions. In addition, corresponding formation and transformation of SOA during photochemical aging was investigated using a large indoor smog chamber. This work would help improve our understanding of primary emission, SOA formation and thus environmental impacts of agricultural residues burning.

2 Materials and methods

2.1 Experimental setup

Photochemical aging was investigated in a smog chamber in the Guangzhou Institute of Geochemistry, Chinese Academy of Sciences (GIG-CAS). The GIG-CAS smog chamber is a ~30 m^3 fluorinated ethylene propylene (FEP) reactor housed in a temperature-controlled room. Details of the chamber setup and associated facilities are provided elsewhere (Wang et al., 2014; Liu et al., 2015, 2016; Deng et al., 2017). Briefly, 135 black lamps (1.2 m long, 60 W Philips, Royal Dutch Philips Electronics Ltd, the Netherlands) are used as light sources, giving a NO_2 photolysis rate of approximately 0.25 min^{-1}. Two Teflon-coated fans are installed inside the reactor to ensure introduced gaseous and particulate species mixed well within 2 min. Prior to each experiment, the reactor was flushed with the purified dry air at a rate of 100 L min^{-1} for at least 48 h. The compressed indoor air is forced through an air dryer (FXe1; Atlas Copco; Sweden) and a series of gas scrubbers containing activated carbon, Purafil, Hopcalite and allochroic silica gel, followed by a PTFE filter to provide the source of the purified air. The purified dry air contains <1 ppb NO_x, O_3 and carbonyl compounds, <5 ppb NMHCs and no detectable particles with relative humidity <5%.

Corn, rice and wheat straws were collected from Henan, Hunan and Guangdong province, respectively. Since moisture content in straws would affect emission factors of atmospheric pollutants (Sanchis et al., 2014; Ni et al., 2015), all the agricultural residues used in this study were dried in a stove at 80 ℃ for 24 h before being burned. After baking, water content in the crop residues was less than 1%. The water content of crop residues was measured by using the method recommended by Liao et al. (2004). The weight of straws were weighed before and after baking in a stove at 105℃ for 24 h, and the difference in weights was calculated to be the weight of the water in the crop residues. Water content was the quotient of the water weight and the whole weight of the straws. In each experiment, ~300 g straws were burned and the burning typically lasted for 3-5 min. Straws were ignited by a butane-fueled lighter and burned under open field burning conditions. The resulting smoke was collected by an inverted funnel and introduced into the chamber using an oil-free pump (Gast Manufacturing, Inc, USA) at a flow rate of ~15 L min^{-1} through a 5.5 m long copper tube (inner diameter: 3/8 inch), and the residence time in the tube was estimated to be <2 s. Before each experiment, the transfer tube was pre-flushed for 15 min with ambient air and 2 min with smokes (not introduced into the chamber reactor). During the whole process, the tube was heated at 80 ℃ to reduce the losses of organic vapors. Based on the volumes of the smoke introduced and the chamber reactor, the dilution ratios were estimated to be 1300-4000, falling into the typical range (1000-10000) under ambient dilution conditions (Robinson et al., 2007). After being characterized in dark for >20 min, black lamps were turned on and the dilute smoke were photochemically aged for 5 h. At the end, black lamps were switched off and the aged aerosols were characterized in the next one hour to determine the particle wall loss. The particle size evolved through the course of photo-oxidation, and the differences in particle wall loss rates during photoreaction and after the lamps were off brought about by the size evolving are estimated to be within ±9% (Figure S1).

In total 20 experiments were conducted (9 for rice straw, 6 for corn straw and 5 for wheat straw), among which 14 experiments were conducted only in the dark to measure primary emissions and 6 experiments were carried out both in the dark and under irradiation to investigate photochemical evolution of open straw burning emissions. Tables 1 and 2 summarize important experimental conditions and key results for all the experiments.

2.2 Instrumentation

Commercial instruments were used for online monitoring of NO_x (EC9841T, Ecotech, Australia), NH_3 (Model 911-0016, Los Gatos Research, USA) and SO_2 (Model 43i, Thermo Scientific, USA). CH_4 and CO were analyzed offline using a gas chromatography (Agilent 6980GC, USA) coupled with a flame ionization detector and a packed column (5A molecular sieve 60/80 mesh, 3 m × 1/8 in) (Zhang et al., 2012), and CO_2 was analyzed using a HP 4890D gas chromatograph (Yi et al., 2007). The detection limits were all less than 30 ppbv for CH_4, CO and CO_2. The relative standard deviations (RSDs) of CO and CO_2 measurements were both less than 3% based on seven duplicate injection of 1.0 ppmv standards (Spectra Gases Inc, USA).Volatile organic compounds (VOCs) were continuously measured using a proton-transfer-reaction time-of-flight mass spectrometer (PTR-TOF-MS; Model 2000, Ionicon Analytik GmbH, Austria). Calibration of the PTR-TOF-MS was performed every few weeks using a certified custom-made standard mixture of VOCs (Ionicon Analytik Gmbh, Austria) that were dynamically diluted to 6 levels (2, 5, 10, 20, 50 and 100 ppbv). Methanol, acetonitrile, acetaldehyde, acrolein, acetone, isoprene, crotonaldehyde, 2-butanone, benzene, toluene, o-xylene, chlorobenzene and α-pinene were included in the calibration mixture. Their sensitivities, indicated by the ratio of the normalized counts per second to the concentration levels of the VOCs in ppbv, were used to convert the raw PTR-TOF-MS signal to concentration (Huang et al., 2016). Quantification of the compounds that were not included in the mixture was performed by using calculated mass-dependent sensitivities based on the measured

194 sensitivities (Stockwell et al., 2015). Mass-dependent sensitivities were linearly fitted for
195 oxygen-containing compounds and the remaining compounds separately. The decay of toluene
196 measured by PTR-TOF-MS was used to derive the OH radical concentrations for every 2 min
197 during each experiment, and the OH exposure was calculated as the product of the OH
198 concentration and the time interval. Continuous monitoring of 20 SOA precursors (including 9
199 NMHCs and 11 oxygen-containing VOCs) from PTR-TOF-MS provided us with data to do the
200 SOA prediction discussed in the Sect 2.3.5 and 3.3.2. Air samples were also collected from the
201 chamber reactor using 2-Liter electro-polished stainless-steel canisters before and after smoke
202 injection. In total 67 C_2-C_{12} NMHCs were measured (Table S1) using an Agilent 5973N gas
203 chromatography mass-selective detector/flame ionization detector (GC-MSD/FID; Agilent
204 Technologies, USA) coupled to a Preconcentrator (Model 7100, Entech Instruments Inc., USA),
205 and analytical procedures have been detailed elsewhere (Wang and Wu, 2008; Zhang et al.,
206 2010; Zhang et al., 2012). Results from GC-MSD/FID were used to quantify the emission
207 factors of 67 NMHCs discussed in the Sect 3.1.
208 Particle number/volume concentrations and size distribution were measured with a
209 scanning mobility particle sizer (SMPS; Classifier model 3080, CPC model 3775, TSI
210 Incorporated, USA). The SMPS was operated with a sheath flow of 3.0 L min^{-1} and a sampling
211 flow of 0.3 L min^{-1}, allowing for a size scanning range of 14 to 760 nm within 255 s. A high-
212 resolution time-of-flight aerosol mass spectrometer (HR-TOF-AMS; Aerodyne Research
213 Incorporated, USA) was used to measure chemical compositions of non-refractory aerosols
214 (DeCarlo et al., 2006). The HR-ToF-AMS was operated by alternating every other min between
215 the high sensitivity V mode and the high resolution W mode. The toolkit Squirrel 1.57I was
216 used to obtain real-time concentration variations of sulfate, nitrate, ammonium, chloride and
217 organics, and the toolkit Pika 1.16I was used to determine the detailed compositions of OA
218 (Aiken et al., 2007, 2008; Canagaratna et al., 2015). The AMS signal at m/z 44 was corrected

for the contribution from gaseous CO_2. The ionization efficiency of the AMS was calibrated routinely by measuring 300 nm monodisperse ammonium nitrate aerosols. Considering the underestimation of particulate matter by the AMS, aerosol mass measured by AMS was corrected with the data from the SMPS and the aethalometer. Conductive silicon tubes were used for aerosol sampling to reduce electrostatic losses of particles.

BC was measured with a seven-channel aethalometer (Model AE-31, Magee Scientific, USA). Cheng et al. (2016) measured the mass absorption efficiency (MAE) of BC from biomass burning at wavelengths of 532 and 1047 nm respectively, and the absorption Ängström exponents (AAE) were estimated to be in the range of 0.9-1.1. Based on relationship between MAE and wavelength, a MAE value of 4.7 m^2 g^{-1} was calculated for 880 nm by assuming the AAE to be 1.0. The MAE value was then applied to convert absorption data in 880 nm to BC mass concentrations. Aethalometer attenuation measurements were corrected for particle loading effects and the scattering of filter fibers using the method developed by Kirchstetter and Novakov (2007) and Schmid et al. (2006).

2.3 Data analysis

2.3.1 Particle effective density

Assuming that particles are spherical and non-porous, the effective density (ρ_{eff}) can be estimated by Eq. (1) (DeCarlo et al. 2004; Schmid et al. 2007):

$$\rho_{eff}=\rho_0 \cdot \frac{d_{va}}{d_m} \qquad (1)$$

where ρ_0 is the standard density (1.0 g cm^{-3}), and d_{va} and d_m are the AMS-measured vacuum aerodynamic diameter and SMPS-measured mobility diameter. The input diameters to this equation were determined by comparing distributions of vacuum aerodynamic and electric mobility diameters, using the AMS and SMPS respectively. Derived ρ_{eff} was used to convert volume concentrations of aerosol particles measured by the SMPS to mass concentrations.

2.3.2 Emission factors and modified combustion efficiency

The carbon mass balance approach (Ward et al., 1992; Andreae and Merlet, 2001) was used to calculate fuel based emission factors (EF) for each compound (g kg^{-1} dry fuel). The emission factor for the *i*th species, EF_i, is calculated by Eq. (2):

$$EF_i = \frac{m_i \cdot EF_C}{\Delta[CO_2]+\Delta[CO]+\Delta[PM_C]+\Delta[HC]} \quad (2)$$

where m_i is the concentration (g m^{-3}) of the *i*th species; $\Delta[CO_2]$, $\Delta[CO]$, and $\Delta[HC]$ are the background-corrected carbon mass concentration (g-C m^{-3}) of the CO_2, CO, and speciated hydrocarbons, respectively; $\Delta[PM_C]$ is the background-corrected carbon in the particle phase (g-C m^{-3}); EF_C is the emission factor of carbon into the air determined by elemental and gravitational analyses, given by Eq. (3):

$$EF_C = \frac{m_{fuel} \cdot \omega_{fuel} - m_{ash} \cdot \omega_{ash}}{m_{fuel}} \quad (3)$$

where ω_{fuel} and ω_{ash} are mass fractions of carbon in the dry fuel and its ash, and m_{fuel} and m_{ash} are the mass of dry fuel and its ash. The modified combustion efficiency (MCE) is defined by Eq. (4) (Heringa et al., 2011; Hennigan et al., 2011; Ni et al., 2015):

$$MCE = \frac{\Delta[CO_2]}{\Delta[CO_2]+\Delta[CO]} \quad (4)$$

2.3.3 Ozone formation potential

The ozone formation potential (OFP) of the speciated NMHCs was calculated from the emission factor and maximum incremental reactivity (MIR) of each individual NMHCs, using Eq. (5):

$$OFP = \sum_{i=1}^{n} (EF_i \cdot MIR_i) \quad (5)$$

where OFP is the ozone formation potential of NMHCs emitted from per unit of biomass (unit: g kg^{-1}), and MIR_i is the MIR of the *i*th NMHC (unit: g O_3 per g NMHC) (Carter, 2008).

2.3.4 Wall loss corrections

Due to the loss of particles and vapors to chamber walls, measured data in chamber studies

need to be corrected for wall loss. For this purpose, in our study one-hour dark decay of aged aerosols was undertaken after photochemical aging was terminated. The loss of particles on the chamber wall is a first-order process (McMurry and Grosjean, 1985). The wall-loss rates of AMS-measured organics, sulfate, nitrate, chloride and ammonium were determined using the dark decay data and were applied to wall-loss correction for the entire experiment. By assuming that the condensed materials on the wall remains completely in equilibrium with the gas phase, we used the ω=1 case to correct the OA mass, where ω is a proportionality factor of organic vapor partitioning to chamber walls and suspended particles (Weitkamp et al., 2007; Henry et al., 2012). For SMPS measurements, the number concentration in each size channel (110 channels in total) was corrected for wall loss separately, since wall loss rates of aerosol particles are size-dependent (Takekawa et al., 2003).

2.3.5 OA production prediction

In this study, twenty NMOGs which have been used to estimate SOA yields by previous work (Ng et al., 2007b; Chan et al., 2009; Hildebrandt et al., 2009; Gómez Alvarez et al., 2009; Chan et al., 2010; Shakya and Griffin, 2010; Chhabra et al., 2011; Nakao et al., 2011; Borras and Tortajada-Genaro, 2012; Yee et al., 2013; Lim et al., 2013) were quantified using PTR-TOF-MS, and the applied SOA yields are summarized in Table S2. The mass concentration of SOA ($[SOA]_{predicted}$, $\mu g\ m^{-3}$) formed from these twenty precursors can be estimated using Eq. (6):

$$[SOA]_{predicted} = \sum_i (\Delta[X_i] \cdot Y_i) \qquad (6)$$

where $\Delta[X_i]$ ($\mu g\ m^{-3}$) is the reacted amount of the *i*th gas-phase precursor and Y_i is the corresponding SOA yield.

Assuming that primary OA (POA) levels kept constant during aging processes, the mass concentration of SOA formed could be estimated as the difference in OA mass concentrations before and after photochemical aging. It should be noted that POA would decrease during aging processes (Tiitta et al., 2016), probably leading to the underestimation of the formed SOA. In

papers where those SOA yields were borrowed from, no organic vapor wall loss were accounted for when calculating the mass concentration of the formed SOA, so the same wall loss correction method was used when comparing the predicted SOA and the formed SOA.

3 Results and discussion

3.1 Emissions of gaseous pollutants

Table 1 compares emission factors of gaseous and particulate species measured in our and previous studies. In our study, emission factors of NO_x were 1.47±0.61, 5.00±3.94, and 3.08±0.93 g kg^{-1} for rice, corn and wheat straw, and NO accounted for 84±11% of NO_x primary emission for all experiments. Emission factors of NH_3 were measured to be 0.45±0.15, 0.63±0.30 and 0.22±0.19 g kg^{-1} for rice, corn and wheat straw. Our measured emission factors of reactive nitrogen species were comparable to those reported by previous studies (Li et al. 2007; Tian et al. 2011). Emission factors of SO_2 were 0.07±0.07, 0.99±1.53 and 0.72±0.34 g kg^{-1} for rice, corn and wheat straw. Our measured emission factors of SO_2 were lower than those reported by Cao et al., (2008) and Kim Oanh et al. (2015) for rice straw, but higher than those reported by Cao et al., (2008) for corn and wheat straw. Due to low sulfur contents in crop straws, the SO_2 emission factors for open burning of crop residues were much lower than those for domestic coal combustion, which were determined to be 2.43-5.36 g kg^{-1} for raw bituminous coal (Du et al., 2016).

Emission factors of the total speciated NMHCs analysed by the GC-MSD/FID system were 5.04±2.04, 2.47±2.11 and 3.08±2.43 g kg^{-1} for rice, corn and wheat straw, respectively (Table 1). Our results were higher than those reported by previous studies (Li et al., 2009; Wang et al., 2014), partly due to the fact that more NMHCs were analyzed in our study (67 species in total). As shown in Figure 1a-c, olefins and acetylene accounted for 56-58% of the total speciated NMHCs, followed by alkanes (22-28%) and aromatic hydrocarbons (16-21%). Table S1 and Figure 2 show the emission factors of each NMHC for open burning of different

straws. Emission factors of unsaturated hydrocarbons ranged from 1.37 (corn) to 2.91 g kg^{-1} (rice), with the majority being ethene, acetylene and propene. Emission factors of alkanes ranged from 0.69 (corn) to 1.09 g kg^{-1} (rice), with ethane and propane being the two most abundant compounds. The emission factors of aromatic hydrocarbons were in the range of 0.42 (corn) to 1.04 (rice), and benzene and toluene are dominant species. It is worth noting that major compounds in the three groups (alkanes, alkenes and aromatic hydrocarbons) were all negatively correlated with the modified combustion efficiency (Figure S2), suggesting that more efficient combustion would reduce their emissions.

Based on their emission factors, we calculated the ozone formation potential for each NMHC. The summed ozone formation potential were 22.5±10.1, 13.7±12.4 and 16.3±13.5 g kg^{-1} for open burning of rice, corn and wheat straw, respectively. As shown in Figure 1d-e, the relative contributions of olefins to the total ozone formation potential could reach >80%. Ethene was the largest ozone precursor (35-42%), followed by propene (16-28%), and these two compounds contributed 58-64% of the total ozone formation potential. Although the emission factors of aromatic hydrocarbons were lower than those of alkanes, their ozone formation potential was dominant over those of alkanes, with toluene being the largest contributor among all the aromatic hydrocarbons. The contribution of alkanes to the total ozone formation potential was minor (2-3%). It is noted that oxygen-containing organic vapors in agricultural residues burning plumes could also have large ozone formation potentials. For example, the OFPs of formaldehyde and acetaldehyde for all experiments were 0.57-2.46 times of the 67 speciated NMHCs.

3.2 Emission of particulate matters

The emission factors of particulate matters were 3.73±3.28, 5.44±3.43, 6.36±2.98 g kg^{-1} for rice, corn and wheat straw, lower than those reported in the previous studies (Table 1). As suggested by Robinson et al. (2007), the POA emission factors would decrease with increasing

dilution ratios, due to evaporation of semi-volatile organic compounds. In this study, the dilution ratios ranged from 1300 to 4000, which were within the typical range of ambient dilution ratios (1000-10000) (Robinson et al. 2007). Therefore, it can be expected that emission factors of primary organic carbon (POC) measured in our study (2.05-4.11 gC kg^{-1}) were lower than those measured by previous work with dilution ratios of 5-20 (Li et al. 2007; Ni et al. 2015). Moreover, it has been shown that the modified combustion efficiency could affect emission factors (Heringa et al., 2011; Stockwell et al., 2015). Figure S3 shows negative correlations of the modified combustion efficiency with emission factors of PM and POC (p<0.05 for both cases), indicating that enhancement of combustion efficiency could reduce the emissions of PM and POC. In our study, all straws were pre-baked to reduce the moisture content to <1%, and this treatment could increase the modified combustion efficiency and thus reduce emission factors of particulate matters (Ni et al., 2015). In addition, the amount of straws burned each time in our experiments was much less than that in the fields, which is expected to avoid oxygen deficit during burning to some extent and thus increase the modified combustion efficiency as well.

While POA emission factors showed large variability for different types of straw, BC emission factors were relatively constant (0.22-0.27 gC kg^{-1}). Since BC is a mixture of non-volatile compounds in particulate matters, as expected, its emission factors measured in our work were comparable to those reported under lower dilution conditions (Li et al. 2007; Ni et al. 2015). The Δ[POA]/Δ[CO] ratios ranged from 0.022 to 0.133 in our study, larger than those (0.001-0.067) measured in chamber studies for hard- and soft-wood fires (Grieshop et al., 2009b) and vegetation commonly burned in North American wildfires (Heringa et al., 2011), but lower than those (0.051-0.329) obtained in field campaigns (Jolleys et al., 2012).

For particle numbers, the emission factors were $(2.94\pm0.91)\times10^{15}$, $(7.29\pm4.17)\times10^{15}$, $(5.87\pm2.89)\times10^{15}$ particle kg^{-1} for rice, corn and wheat straw, respectively (Table 1). Our results

were comparable to that (1×10^{15} particle kg^{-1}) for crop residues burning (Andreae and Merlet, 2001) and those (3.2×10^{15}-10.9×10^{15} particle kg^{-1}) for wood burning (Hosseini et al., 2013) but two magnitudes larger than those for crop residues burning in a sealed stove (Zhang et al. 2008).

3.3 Evolution of particles

3.3.1 Growth of particle size

Figure 3 shows the evolution of particle size distribution after photochemical aging of 0, 0.5, 2.5 and 5 h. Aerosol particles emitted from open straw burning were peaked at 50-90 nm under ambient dilution conditions. The geometric mean diameters for primarily emitted particles in this study were smaller than those (100-150 nm) reported for crop residuals burning under low dilution conditions (Zhang et al., 2011; Li et al., 2015), probabley due to evaporation of organic vapors under the high dilution conditions (Lipsky et al., 2006) and coagulation of fine particles under the low dilution conditions (Hossain et al., 2012).

After switching on black lamps, apparent growth of particle size was observed. In all the aging experiments, growth rates of particle diameters in the first 0.5 h were 10 times larger than those afterwards, and after 5 h aging the geometric mean diameters peaked at 60-120 nm. For instance, in the photochemical aging experiment for wheat straw burning (Figure 3c), the growth rate of particles was 18 nm h^{-1} in the first 0.5 h and decreased to ~1 nm h^{-1} during the following 4.5 h. The size distribution of aged aerosol particles in our study is similar to those of ambient particles under the severe biomass burning impact during haze events (Betha et al., 2014; Niu et al., 2016).

3.3.2 Particle mass enhancement

Figure 4 shows the chemical evolution of aerosol particles during the 5 h photochemical aging of wheat straw burning. During the whole process, OA kept increasing and was dominant over inorganic species. After 3 h of photochemical aging, the levels of all the inorganic species were constant, and nitrate was the second most abundant component with a mass fraction of 7%,

followed by chloride (2%), ammonium (1%) and sulfate (<1%). Figure 4b depicts [OA] evolution as a function of OH exposure. OA increased slowly at the first ~0.2 h, and then increased rapidly with OH exposure.

The OA enhancement ratio, defined as the mass ratio of aged OA at the end of each aging experiment to POA, was calculated. In the six aging experiments, the OH exposure and OA enhancement ratios ranged from (1.87-4.97)×10^{10} molecule cm^{-3} s and 2.4-7.6, respectively. Assuming an average OH concentration of 1.5×10^{6} molecule cm^{-3} in the ambient air (Hayes et al., 2013), this means that rapid SOA formation would occur in 3.5-9.2 h during the daytime after straw burning. The OA enhancement ratios determined in our study were higher than those (0.7-2.9) for the combustion of vegetation commonly burned in North American wildfires (Hennigan et al., 2011), and comparable to those (0.7-6.9) for wood burning (Grieshop et al., 2009b; Heringa et al., 2011).

Recently, Bruns et al., (2016) found that 22 NMOGs emitted from residential wood burning could explain the majority of the formed SOA. In our study, 20 of the 22 NMOGs were detected and quantified with the PTR-TOF-MS. Concentration differences of each compound before and after photo-oxidation were calculated to estimate the SOA formed from these precursors. Since SOA formation highly depends on oxidation conditions, SOA yields for a certain precursor vary with VOC/NO_x ratios. In our work, we chose a set of SOA yields for these NMOGs based on the observed VOC/NO_x ratio in the chamber experiments. More specifically, if the observed VOC/NO_x ratio for a certain precursor in the chamber was within the VOC/NO_x range reported in literature, the mean value of the highest and lowest yields within the VOC/NO_x range in literature was used to estimate the SOA formed from the precursor in the chamber; if the observed VOC/NO_x ratio for a certain precursor was higher than the maximum VOC/NO_x ratio reported in literature, we chose the yield reported at the maximum VOC/NO_x ratio; if the observed VOC/NO_x ratio was lower than the minimum

417 VOC/NO_x ratio reported in literature, we chose the yield reported at the minimum VOC/NO_x
418 ratio.

419 Figure 5a shows the time series of POA, $SOA_{predicted}$ and unexplained SOA in a typical
420 aging experiment. The contribution of $SOA_{predicted}$ by the 20 NMOGs was minor, and large
421 fractions of observed SOA could not be explained. In all the experiments, only 5.0-27.3% of
422 the observed SOA mass could be explained by the 20 NMOGs (Figure 5b). Even if the highest
423 SOA yield for each precursor reported in literature was used, 60-90% of observed SOA mass
424 still could not be explained. It has been suggested that aqueous-phase oxidation of alkenes
425 could produce substantial SOA (Ervens et al., 2011). Considering large emissions of olefins
426 from straw burning (Figure 1a-c), we also estimated the SOA formed from the three most
427 abundant alkenes (ethene, acetylene, and propene) with their newly-developed SOA yields (Ge
428 et al., 2016; Jia and Xu, 2016; Ge et al., 2017), and their total contribution to the observed SOA
429 was found to be negligible (<0.5%). It is noted that although over 80 VOCs species were
430 quantified by the GC-MSD/FID and the PTR-TOF-MS in this study, only 20 species among
431 them were taken into the SOA prediction because of the lack of published data for SOA yields.
432 The unaccounted VOC species might be a reason for the discrepancy. On the other hand, as
433 indicated by Deng et al. (2017), SOA yields obtained from chamber studies in purified air
434 matrix might be lower than that in real ambient air matrix. Consequently, using SOA yields
435 from studies in purified air matrix might also under predict SOA yields in the complex biomass
436 burning plume matrix. Moreover, oxidation of particulate organic matters (POM), like semi-
437 volatile organic compounds (SVOC) and intermediate volatility organic compounds (IVOC),
438 would also contribute substantially to SOA formation (Presto et al., 2009; Zhao et al., 2014),
439 yet this is not accounted for in our prediction. Above all, there are still unknown precursors
440 and/or physicochemical processes contributing the majority of SOA formed from open straw
441 burning.

3.3.3 OA mass spectrum evolution

In the high resolution W mode of AMS, ions generated from particles could be identified by their exact mass-charge ratio (m/z) and then grouped into CHON, CHO, CHN and CH families. Figure 6 presents the evolution of OA mass spectra. For POA (Figure 6a), CH-family was the major component with a mass fraction of 68%, followed by CHO (23%), CHN (6%), and CHON (2%). The ions at m/z 43, 41 and 55 were the dominant peaks in the POA mass spectrum. The major ions at m/z 27, 39, 41, 55, 57, 67 and 69 belonged to the CH-family and could be the fragments of hydrocarbons (Weimer et al., 2008). The peaks at m/z 28, 29, 43, 44 and 55 contained considerable CHO ions, and the corresponding ions (CO^+, CHO^+, $C_2H_3O^+$, CO_2^+ and $C_3H_3O^+$) could be the fragments of aldehydes, ketones and carboxylic acid (Ng et al., 2011a). The peak at m/z 91 was mainly attributed to $C_7H_7^+$, possibly originating from aromatic compounds.

The mass spectra of aged OA was quite different from that of POA (Figure 6b-c). The mass fraction of the CH-family decreased to 46% and was comparable to that of CHO-family, while the contribution of N-containing OA (CHN and CHON) increased to ~11%. The ions at m/z 44 and 43, mainly coming from the CHO-family, became the dominant peaks for the aged OA. The fractions of two major masses at m/z 44 (f_{44}) and m/z 43 (f_{43}) in OA can be used to generate an f_{44} vs. f_{43} triangular space, in which oxygenated organic aerosol (OOA) moves towards the apex during the aging process (Ng et al., 2010). In addition, f_{44} in the ambient air was suggested to be 0.07±0.04 for semi-volatile OOA (SV-OOA) and 0.17±0.04 for low-volatility OOA (LV-OOA), respectively (Ng et al., 2010). Figure 7a plots f_{44} and f_{43} of the POA and the aged OA in all the six experiments. Most of data are within the f_{44} vs. f_{43} triangular space and close to the left margin. Photochemical aging led to increase in f_{44} for all the experiments, suggesting transformation of OA from SV-OOA to LV-OOA. For comparison, the f_{43} did not change significantly in all the experiments. The main ions at m/z 43 were $C_2H_3O^+$ and $C_3H_7^+$. It can be

observed in Figure 6c that the increased contribution of $C_2H_3O^+$ and the decrease contribution of $C_3H_7^+$ were comparable during photoreaction.

The ion at m/z 60, mainly consisting of $C_2H_4O_2^+$, is regarded as a BBOA marker, and the mass fraction of this ion in OA, f_{60}, is widely used to probe the evolution of BBOA (Brito et al., 2014; May et al., 2015). Figure 7b plots evolution of f_{44} and f_{60} in all the experiments conducted in this study, in order to compare with measurements in aging biomass burning plumes (Cubison et al., 2011) and those in the POA from different types of biomass burning (Alfarra et al., 2007; Brito et al., 2014; May et al., 2015). Photo-oxidation caused increase in f_{44} and decrease in f_{60}, and this is consistent with the general evolution of OA in ambient biomass burning plumes (Cubison et al., 2011). However, our measured f_{60}, 0.003-0.006 in the POA from open straw burning and 0.002-0004 in aged OA, were all lower than those from other field campaigns and quite near the background f_{60} level of 0.003 for ambient OA (Cubison et al., 2011; Figure 7b). Low values of f_{60} (0.005-0.02) were also reported by Hennigan et al. (2011) in a chamber study for fuels commonly burned in wildfires. In their study, biomass burning took place in a 3000 m^3 combustion chamber, and the smokes were then injected into another chamber for aging experiments with a dilution ratio of ~25. Previous studies have demonstrated that levoglucosan is a semi-volatile compound with a saturation concentration of ~8 μg m^{-3} at 293 K (Grieshop et al., 2009b; Huffman et al., 2009; Hennigan et al. 2011). As a result, high dilution conditions used in our study would cause levoglucosan to evaporate, and this may at least partly explain the low f_{60} observed in the POA from straw burning. From previous studies, the levoglucosan/OC ratios of straw burning ranging from 4.92 to 16.8% (4 types of vegetation summarized; Dhammapala et al., 2007; Kim Oanh et al., 2011; Hall et al., 2012) were not significantly (two-sample t-test, p>0.05) lower than those of prescribed fuel burning, wildfire and wood burning ranging from 1.46 to 13.5% (20 types of vegetation summarized; Hosseini et al., 2013; Shahid et al., 2015). So the difference in fuel type cannot

492 explain the lower f_{60} observed in our study.

493 **3.3.4 Elemental ratio and oxidation state of OA**

494 In this study, the O/C and H/C ratios in the POA from different straws burning were in the
495 range of 0.20-0.38 and 1.58-1.74, respectively. After 5 h aging, O/C increased and H/C
496 decreased (Table 2). Kroll et al. (2011) proposed a metric, the average carbon oxidation state
497 (OS_c), to describe the degree of oxidation of atmospheric organic species. OS_c could be
498 calculated from the elemental composition of OA measured by AMS, given by Eq. (7):

499 $$OS_c = 2 \times O/C - H/C \qquad (7)$$

500 In this study, the OS_c values for the fresh POA from open straw burning ranged from -
501 1.25 to -0.89, consistent with those suggested for BBOA (-1 to -0.7) (Kroll et al. 2011). During
502 photochemical aging, the OS_c values increased linearly (p<0.001) with OH exposure (Figure
503 8), and the slopes were quite near each other even for different types of straws, implying AMS
504 measured OS_c might be a good indicator of OH exposure and thereby of photochemical aging.

505 Figure 9 shows the Van Krevelen diagram of OA. In this study, the slopes of linear
506 correlations between H/C and O/C range from -0.49 to -0.24 for the five experiments. Slopes
507 of -1, 0.5 and 0 in the Van Krevelen diagrams indicate addition of carboxylic acids without
508 fragmentation, addition of carboxylic acids with fragmentation, and addition of
509 alcohols/peroxides, respectively (Heald et al., 2010; Ng et al., 2011a). Therefore, the slopes
510 determined in our study suggest that open straw burning OA aging resulted in net changes in
511 chemical composition equivalent to addition of carboxylic acid groups with C-C bond breakage
512 and addition of alcohol/peroxide functional groups.

513 **4 Conclusion**

514 In this study, primary emissions of open burning of rice, corn and wheat straw and their
515 photochemical were investigated using a large indoor chamber. Emission factors of NO_x, NH_3,
516 SO_2, 67 NMHCs, PM and particle number were measured under dilution ratios ranging from

517 1300 to 4000. Emission factors of PM (3.73-6.36 g kg^{-1}) and POC (2.05-4.11 gC kg^{-1}) were
518 lower than those reported in previous studies conducted at lower dilution ratios, probably due
519 to the evaporation of semi-volatile organic compounds. Emission factors of POC, PM and
520 major NMHCs compounds were all negatively correlated with the modified combustion
521 efficiency, suggesting that incomplete burning of agricultural residues could lead to larger
522 primary emission.

523 Both agricultural residues burning and domestic coal combustion have been recognized
524 to contribute substantially to the deteriorating regional air quality especially in rural areas of
525 China (Pan et al., 2015; Liu et al., 2016; Zhu et al., 2016). The emission factors of the speciated
526 NMHCs, PM, NO_x, CO and SO_2 from combustion of raw bituminous, which is currently
527 prevailing for cooking and heating in rural areas, have been reported to be 0.56-5.40,
528 25.49±2.30, 0.97±0.03, 208±5 and 2.43-5.36 g kg^{-1}, respectively (Du et al., 2016; Li et al.,
529 2016; Liu et al., 2017). Annually burned crop residues and domestic coals were estimated to
530 be 160 Tg (Li et al., 2016) and 99.6 Tg (NBSPRC, 2014) in China. Therefore, with the emission
531 factors of the speciated NMHCs (2.47-5.04 g kg^{-1}), PM (3.73-6.36 g kg^{-1}), NO_x (1.47-5.00 g
532 kg^{-1}), CO (46.1-63.5 g kg^{-1}) and SO_2 (0.07-0.99 g kg^{-1}) measured for agricultural residues
533 burning in this study, agricultural residues burning might emit more NMHCs and NO_x, but less
534 primary PM, CO and SO_2 than domestic coal burning on a national scale.

535 Photochemical aging of primary emissions was investigated with OH exposure equal to
536 3.2-9.2 hours under typical ambient conditions, and at the end of experiments the OA mass
537 concentrations increased by a factor of 2.4-7.6, suggesting that SOA could be rapidly produced
538 within several hours. Our estimation suggests that phenols are the most important identified
539 SOA precursors, and more than 70% of the formed OA still cannot be explained by the
540 oxidation of known precursors. Measurements using HR-TOF-AMS reveal that after
541 photochemical aging, signals for oxygen- and nitrogen-containing compounds were largely

increased, with OS_c increased in a highly significant linear way with OH exposure.

Acknowledgements

This study was supported by Strategic Priority Research Program of the Chinese Academy of Sciences (Grant No. XDB05010200), National Natural Science Foundation of China (Grant No. 41530641/41571130031/41673116/41503105), National Key Research and Development Program (2016YFC0202204) and Guangzhou Science Technology and Innovation Commission (201505231532347).

References

Adler, G., Flores, J. M., Riziq, A. A., Borrmann, S., and Rudich, Y.: Chemical, physical, and optical evolution of biomass burning aerosols: a case study, Atmos. Chem. Phys., 11, 1491-1503, doi:10.5194/acp-11-1491-2011, 2011.

Aiken, A. C., DeCarlo, P. F., and Jimenez, J. L.: Elemental analysis of organic species with electron ionization high-resolution mass spectrometry, Anal. Chem., 79, 8350-8358, doi:10.1021/ac071150w, 2007.

Aiken, A. C., Decarlo, P. F., Kroll, J. H., Worsnop, D. R., Huffman, J. A., Docherty, K. S., Ulbrich, I. M., Mohr, C., Kimmel, J. R., Sueper, D., Sun, Y., Zhang, Q., Trimborn, A., Northway, M., Ziemann, P. J., Canagaratna, M. R., Onasch, T. B., Alfarra, M. R., Prevot, A. S. H., Dommen, J., Duplissy, J., Metzger, A., Baltensperger, U., and Jimenez, J. L.: O/C and OM/OC ratios of primary, secondary, and ambient organic aerosols with high-resolution time-of-flight aerosol mass spectrometry, Environ. Sci. Technol., 42, 4478-4485, doi:10.1021/es703009q, 2008.

Akagi, S. K., Yokelson, R. J., Wiedinmyer, C., Alvarado, M. J., Reid, J. S., Karl, T., Crounse, J. D., and Wennberg, P. O.: Emission factors for open and domestic biomass burning for

use in atmospheric models, Atmos. Chem. Phys., 11, 4039-4072, doi:10.5194/acp-11-4039-2011, 2011.

Alfarra, M. R., Prevot, A. S. H., Szidat, S., Sandradewi, J., Weimer, S., Lanz, V. A., Schreiber, D., Mohr, M., and Baltensperger, U.: Identification of the mass spectral signature of organic aerosols from wood burning emissions, Environ. Sci. Technol., 41, 5770-5777, doi:10.1021/es062289b, 2007.

Alves, N. d. O., Brito, J., Caumo, S., Arana, A., Hacon, S. d. S., Artaxo, P., Hillamo, R., Teinila, K., Batistuzzo de Medeiros, S. R., and Vasconcellos, P. d. C.: Biomass burning in the Amazon region: Aerosol source apportionment and associated health risk assessment, Atmos. Environ., 120, 277-285, doi:10.1016/j.atmosenv.2015.08.059, 2015.

Andreae, M. O., and Merlet, P.: Emission of trace gases and aerosols from biomass burning, Global Biogeochem. Cy., 15, 955-966, doi:10.1029/2000GB001382, 2001.

Andreae, M. O., Rosenfeld, D., Artaxo, P., Costa, A. A., Frank, G. P., Longo, K. M., and Silva-Dias, M. A. F.: Smoking Rain Clouds over the Amazon, Science, 303, 1337-1342, doi:10.1126/science.1092779, 2004.

Arnold, S. R., Emmons, L. K., Monks, S. A., Law, K. S., Ridley, D. A., Turquety, S., Tilmes, S., Thomas, J. L., Bouarar, I., Flemming, J., Huijnen, V., Mao, J., Duncan, B. N., Steenrod, S., Yoshida, Y., Langner, J., and Long, Y.: Biomass burning influence on high-latitude tropospheric ozone and reactive nitrogen in summer 2008: a multi-model analysis based on POLMIP simulations, Atmos. Chem. Phys., 15, 6047-6068, doi:10.5194/acp-15-6047-2015, 2015.

Betha, R., Zhang, Z., and Balasubramanian, R.: Influence of trans-boundary biomass burning impacted air masses on submicron particle number concentrations and size distributions, Atmos. Environ., 92, 9-18, doi:10.1016/j.atmosenv.2014.04.002, 2014.

Bond, T. C., Doherty, S. J., Fahey, D. W., Forster, P. M., Berntsen, T., DeAngelo, B. J., Flanner,

592 M. G., Ghan, S., Kaercher, B., Koch, D., Kinne, S., Kondo, Y., Quinn, P. K., Sarofim, M.
593 C., Schultz, M. G., Schulz, M., Venkataraman, C., Zhang, H., Zhang, S., Bellouin, N.,
594 Guttikunda, S. K., Hopke, P. K., Jacobson, M. Z., Kaiser, J. W., Klimont, Z., Lohmann,
595 U., Schwarz, J. P., Shindell, D., Storelvmo, T., Warren, S. G., and Zender, C. S.: Bounding
596 the role of black carbon in the climate system: A scientific assessment, J. Geophys. Res.-
597 Atmos., 118, 5380-5552, doi:10.1002/jgrd.50171, 2013.
598 Bond, T. C., Streets, D. G., Yarber, K. F., Nelson, S. M., Woo, J. H., and Klimont, Z.: A
599 technology-based global inventory of black and organic carbon emissions from
600 combustion, J. Geophys. Res.-Atmos., 109, 43, doi:10.1029/2003jd003697, 2004.
601 Borras, E., and Tortajada-Genaro, L. A.: Secondary organic aerosol formation from the photo-
602 oxidation of benzene, Atmos. Environ., 47, 154-163, doi:10.1016/j.atmosenv.2011.11.020,
603 2012.
604 Brassard, P., Palacios, J. H., Godbout, S., Bussieres, D., Lagace, R., Larouche, J. P., and
605 Pelletier, F.: Comparison of the gaseous and particulate matter emissions from the
606 combustion of agricultural and forest biomasses, Bioresour. Technol., 155, 300-306,
607 doi:10.1016/j.biortech.2013.12.027, 2014.
608 Brito, J., Rizzo, L. V., Morgan, W. T., Coe, H., Johnson, B., Haywood, J., Longo, K., Freitas,
609 S., Andreae, M. O., and Artaxo, P.: Ground-based aerosol characterization during the
610 South American Biomass Burning Analysis (SAMBBA) field experiment, Atmos. Chem.
611 Phys., 14, 12069-12083, doi:10.5194/acp-14-12069-2014, 2014.
612 Bruns, E. A., El Haddad, I., Slowik, J. G., Kilic, D., Klein, F., Baltensperger, U., and Prevot,
613 A. S. H.: Identification of significant precursor gases of secondary organic aerosols from
614 residential wood combustion, Sci. Rep., 6, doi:10.1038/srep27881, 2016.
615 Bruns, E. A., Slowik, J. G., El Haddad, I., Kilic, D., Klein, F., Dommen, J., Temime-Roussel,
616 B., Marchand, N., Baltensperger, U., and Prevot, A. S. H.: Characterization of gas-phase

organics using proton transfer reaction time-of-flight mass spectrometry: fresh and aged residential wood combustion emissions, Atmos. Chem. Phys., 17, 705-720, doi:10.5194/acp-17-705-2017, 2017.

Canagaratna, M. R., Jimenez, J. L., Kroll, J. H., Chen, Q., Kessler, S. H., Massoli, P., Hildebrandt Ruiz, L., Fortner, E., Williams, L. R., Wilson, K. R., Surratt, J. D., Donahue, N. M., Jayne, J. T., and Worsnop, D. R.: Elemental ratio measurements of organic compounds using aerosol mass spectrometry: characterization, improved calibration, and implications, Atmos. Chem. Phys., 15, 253-272, doi:10.5194/acp-15-253-2015, 2015.

Cao, G., Zhang, X., Gong, S., and Zheng, F.: Investigation on emission factors of particulate matter and gaseous pollutants from crop residue burning, J. Environ. Sci., 20, 50-55, doi:10.1016/S1001-0742(08)60007-8, 2008.

Carter, W. P. L.: Reactivity estimates for selected consumer product compounds, Air resources Board, California, Contract No. 06-408, 72-99, 2008.

Chan, A. W. H., Kautzman, K. E., Chhabra, P. S., Surratt, J. D., Chan, M. N., Crounse, J. D., Kürten, A., Wennberg, P. O., Flagan, R. C., and Seinfeld, J. H.: Secondary organic aerosol formation from photooxidation of naphthalene and alkylnaphthalenes: implications for oxidation of intermediate volatility organic compounds (IVOCs), Atmos. Chem. Phys., 9, 3049-3060, doi:10.5194/acp-9-3049-2009, 2009.

Chan, A. W. H., Chan, M. N., Surratt, J. D., and Chhabra, P. S.: Role of aldehyde chemistry and NO_x concentrations in secondary organic aerosol formation, Atmos. Chem. Phys., 10, 7169-7188, doi:10.5194/acp-10-7169-2010, 2010.

Cheng, Y., Engling, G., He, K. B., Duan, F. K., Ma, Y. L., Du, Z. Y., Liu, J. M., Zheng, M., and Weber, R. J.: Biomass burning contribution to Beijing aerosol, Atmos. Chem. Phys., 13, 7765-7781, doi:10.5194/acp-13-7765-2013, 2013.

Cheng, Y., Engling, G., Moosmaller, H., Arnott, W. P., Chen, L. W. A., Wold, C. E., Hao, W.

642 M., and He, K. B.: Light absorption by biomass burning source emissions, Atmos.
643 Environ., 127, 347-354, doi:10.1016/j.atmosenv.2015.12.045, 2016.
644 Chhabra, P. S., Ng, N. L., Canagaratna, M. R., Corrigan, A. L., Russell, L. M., Worsnop, D. R.,
645 Flagan, R. C., and Seinfeld, J. H.: Elemental composition and oxidation of chamber
646 organic aerosol, Atmos. Chem. Phys., 11, 8827-8845, doi:10.5194/acp-11-8827-2011,
647 2011.
648 Christian, T. J., Yokelson, R. J., Cardenas, B., Molina, L. T., Engling, G., and Hsu, S. C.: Trace
649 gas and particle emissions from domestic and industrial biofuel use and garbage burning
650 in central Mexico, Atmos. Chem. Phys., 10, 565-584, doi:10.5194/acp-10-565-2010, 2010.
651 Cubison, M. J., Ortega, A. M., Hayes, P. L., Farmer, D. K., Day, D., Lechner, M. J., Brune, W.
652 H., Apel, E., Diskin, G. S., Fisher, J. A., Fuelberg, H. E., Hecobian, A., Knapp, D. J.,
653 Mikoviny, T., Riemer, D., Sachse, G. W., Sessions, W., Weber, R. J., Weinheimer, A. J.,
654 Wisthaler, A., and Jimenez, J. L.: Effects of aging on organic aerosol from open biomass
655 burning smoke in aircraft and laboratory studies, Atmos. Chem. Phys., 11, 12049-12064,
656 doi:10.5194/acp-11-12049-2011, 2011.
657 DeCarlo, P. F., Slowik, J. G., Worsnop, D. R., Davidovits, P., and Jimenez, J. L.: Particle
658 morphology and density characterization by combined mobility and aerodynamic
659 diameter measurements. Part 1: Theory, Aerosol Sci. Technol., 38, 1185-1205,
660 doi:10.1080/027868290903907, 2004.
661 DeCarlo, P. F., Kimmel, J. R., Trimborn, A., Northway, M. J., Jayne, J. T., Aiken, A. C., Gonin,
662 M., Fuhrer, K., Horvath, T., Docherty, K. S., Worsnop, D. R., and Jimenez, J. L.: Field-
663 deployable, high-resolution, time-of-flight aerosol mass spectrometer, Anal. Chem., 78,
664 8281-8289, doi:10.1021/ac061249n, 2006.
665 Deng, W., Liu, T., Zhang, Y., Situ, S., Hu, Q., He, Q., Zhang, Z., Lü, S., Bi, X., Wang, X.,
666 Boreave, A., George, C., Ding, X., and Wang, X.: Secondary organic aerosol formation

667 from photo-oxidation of toluene with NO_x and SO_2: Chamber simulation with purified air
668 versus urban ambient air as matrix, Atmos. Environ., 150, 67-76,
669 doi:10.1016/j.atmosenv.2016.11.047, 2017.
670 Dhammapala, R., Claiborn, C., Jimenez, J., Corkill, J., Gullett, B., Simpson, C., and Paulsen,
671 M.: Emission factors of PAHs, methoxyphenols, levoglucosan, elemental carbon and
672 organic carbon from simulated wheat and Kentucky bluegrass stubble burns, Atmos.
673 Environ., 41, 2660-2669, doi:10.1016/j.atmosenv.2006.11.023, 2007.
674 Ding, X., He, Q.-F., Shen, R.-Q., Yu, Q.-Q., Zhang, Y.-Q., Xin, J.-Y., Wen, T.-X., and Wang,
675 X.-M.: Spatial and seasonal variations of isoprene secondary organic aerosol in China:
676 Significant impact of biomass burning during winter, Sci. Rep., 6, 20411,
677 doi:10.1038/srep20411, 2016a.
678 Ding, X., Zhang, Y.-Q., He, Q.-F., Yu, Q.-Q., Shen, R.-Q., Zhang, Y., Zhang, Z., Lyu, S.-J., Hu,
679 Q.-H., Wang, Y.-S., Li, L.-F., Song, W., and Wang, X.-M.: Spatial and seasonal variations
680 of secondary organic aerosol from terpenoids over China, J. Geophys. Res.-Atmos., 121,
681 14661–14678, doi:10.1002/2016JD025467, 2016b.
682 Ding, X., Zhang, Y.-Q., He, Q.-F., Yu, Q.-Q., Wang, J.-Q., Shen, R.-Q., Song, W., Wang, Y.-S.,
683 and Wang, X.-M.: Significant increase of aromatics-derived secondary organic aerosol
684 during fall to winter in China, Environ. Sci. Technol., doi:10.1021/acs.est.6b06408, 2017.
685 Du, Q., Zhang, C., Mu, Y., Cheng, Y., Zhang, Y., Liu, C., Song, M., Tian, D., Liu, P., Liu, J.,
686 Xue, C., and Ye, C.: An important missing source of atmospheric carbonyl sulfide:
687 Domestic coal combustion, Geophys. Res. Lett., 43, 8720-8727,
688 doi:10.1002/2016gl070075, 2016.
689 Duncan, B. N., Bey, I., Chin, M., Mickley, L. J., Fairlie, T. D., Martin, R. V., and Matsueda, H.:
690 Indonesian wildfires of 1997: Impact on tropospheric chemistry, J. Geophys. Res.-Atmos.,
691 108, 25, doi:10.1029/2002jd003195, 2003.

692 Ervens, B., Turpin, B. J., and Weber, R. J.: Secondary organic aerosol formation in cloud
693 droplets and aqueous particles (aqSOA): a review of laboratory, field and model studies,
694 Atmos. Chem. Phys., 11, 11069-11102, doi:10.5194/acp-11-11069-2011, 2011.
695 Food and Agriculture Organization of the United Nation: Emissions of methane and nitrous
696 oxide from the on-site combustion of crop residues,
697 http://faostat3.fao.org/browse/G1/GB/E, last accessed: 6 April 2017.
698 Ge, S., Xu, Y., and Jia, L.: Secondary organic aerosol formation from ethyne in the presence of
699 NaCl in a smog chamber, Environ. Chem., 13, 699-710, doi:10.1071/en15155, 2016.
700 Ge, S., Xu, Y., and Jia, L.: Secondary organic aerosol formation from propylene irradiations in
701 a chamber study, Atmos. Environ., 157, 146-155, doi:10.1016/j.atmosenv.2017.03.019,
702 2017.
703 Giordano, M. R., Short, D. Z., Hosseini, S., Lichtenberg, W., and Asa-Awuku, A. A.: Changes
704 in droplet surface tension affect the observed hygroscopicity of photochemically aged
705 biomass burning aerosol, Environ. Sci. Technol., 47, 10980-10986,
706 doi:10.1021/es401867j, 2013.
707 Gómez Alvarez, E., Borras, E., Viidanoja, J., and Hjorth, J.: Unsaturated dicarbonyl products
708 from the OH-initiated photo-oxidation of furan, 2-methylfuran and 3-methylfuran, Atmos.
709 Environ., 43, 1603-1612, doi:10.1016/j.atmosenv.2008.12.019, 2009.
710 Grieshop, A. P., Donahue, N. M., and Robinson, A. L.: Laboratory investigation of
711 photochemical oxidation of organic aerosol from wood fires 2: analysis of aerosol mass
712 spectrometer data, Atmos. Chem. Phys., 9, 2227-2240, doi:10.5194/acp-9-2227-2009,
713 2009a.
714 Grieshop, A. P., Logue, J. M., Donahue, N. M., and Robinson, A. L.: Laboratory investigation
715 of photochemical oxidation of organic aerosol from wood fires 1: measurement and
716 simulation of organic aerosol evolution, Atmos. Chem. Phys., 9, 1263-1277,

717 doi:10.5194/acp-9-1263-2009, 2009b.
718 Hall, D., Wu, C. Y., Hsu, Y. M., Stormer, J., Engling, G., Capeto, K., Wang, J., Brown, S., Li,
719 H. W., and Yu, K. M.: PAHs, carbonyls, VOCs and $PM_{2.5}$ emission factors for pre-harvest
720 burning of Florida sugarcane, Atmos. Environ., 55, 164-172,
721 doi:10.1016/j.atmosenv.2012.03.034, 2012.
722 Hatch, L. E., Yokelson, R. J., Stockwell, C. E., Veres, P. R., Simpson, I. J., Blake, D. R., Orlando,
723 J. J., and Barsanti, K. C.: Multi-instrument comparison and compilation of non-methane
724 organic gas emissions from biomass burning and implications for smoke-derived
725 secondary organic aerosol precursors, Atmos. Chem. Phys., 17, 1471-1489,
726 doi:10.5194/acp-17-1471-2017, 2017.
727 Hayes, P. L., Ortega, A. M., Cubison, M. J., Froyd, K. D., Zhao, Y., Cliff, S. S., Hu, W. W.,
728 Toohey, D. W., Flynn, J. H., Lefer, B. L., Grossberg, N., Alvarez, S., Rappenglueck, B.,
729 Taylor, J. W., Allan, J. D., Holloway, J. S., Gilman, J. B., Kuster, W. C., De Gouw, J. A.,
730 Massoli, P., Zhang, X., Liu, J., Weber, R. J., Corrigan, A. L., Russell, L. M., Isaacman, G.,
731 Worton, D. R., Kreisberg, N. M., Goldstein, A. H., Thalman, R., Waxman, E. M.,
732 Volkamer, R., Lin, Y. H., Surratt, J. D., Kleindienst, T. E., Offenberg, J. H., Dusanter, S.,
733 Griffith, S., Stevens, P. S., Brioude, J., Angevine, W. M., and Jimenez, J. L.: Organic
734 aerosol composition and sources in Pasadena, California, during the 2010 CalNex
735 campaign, J. Geophys. Res.-Atmos., 118, 9233-9257, doi:10.1002/jgrd.50530, 2013.
736 Heald, C. L., Kroll, J. H., Jimenez, J. L., Docherty, K. S., DeCarlo, P. F., Aiken, A. C., Chen,
737 Q., Martin, S. T., Farmer, D. K., and Artaxo, P.: A simplified description of the evolution
738 of organic aerosol composition in the atmosphere, Geophys. Res. Lett., 37, L08803,
739 doi:10.1029/2010gl042737, 2010.
740 Hennigan, C. J., Miracolo, M. A., Engelhart, G. J., May, A. A., Presto, A. A., Lee, T., Sullivan,
741 A. P., McMeeking, G. R., Coe, H., Wold, C. E., Hao, W. M., Gilman, J. B., Kuster, W. C.,

742 de Gouw, J., Schichtel, B. A., Collett, J. L., Kreidenweis, S. M., and Robinson, A. L.:
743 Chemical and physical transformations of organic aerosol from the photo-oxidation of
744 open biomass burning emissions in an environmental chamber, Atmos. Chem. Phys., 11,
745 7669-7686, doi:10.5194/acp-11-7669-2011, 2011.
746 Henry, K. M., Lohaus, T., and Donahue, N. M.: Organic aerosol yields from α-pinene oxidation:
747 bridging the gap between first-generation yields and aging chemistry, Environ. Sci.
748 Technol., 46, 12347-12354, doi:10.1021/es302060y, 2012.
749 Heringa, M. F., DeCarlo, P. F., Chirico, R., Tritscher, T., Dommen, J., Weingartner, E., Richter,
750 R., Wehrle, G., Prévôt, A. S. H., and Baltensperger, U.: Investigations of primary and
751 secondary particulate matter of different wood combustion appliances with a high-
752 resolution time-of-flight aerosol mass spectrometer, Atmos. Chem. Phys., 11, 5945-5957,
753 doi:10.5194/acp-11-5945-2011, 2011.
754 Hildebrandt, L., Donahue, N. M., and Pandis, S. N.: High formation of secondary organic
755 aerosol from the photo-oxidation of toluene, Atmos. Chem. Phys., 9, 2973-2986,
756 doi:10.5194/acp-9-2973-2009, 2009.
757 Hossain, A., Park, S., Kim, J. S., and Park, K.: Volatility and mixing states of ultrafine particles
758 from biomass burning, J. Hazard. Mater., 205, 189-197,
759 doi:10.1016/j.jhazmat.2011.12.061, 2012.
760 Hosseini, S., Urbanski, S. P., Dixit, P., Qi, L., Burling, I. R., Yokelson, R. J., Johnson, T. J.,
761 Shrivastava, M., Jung, H. S., Weise, D. R., Miller, J. W., and Cocker, D. R.: Laboratory
762 characterization of PM emissions from combustion of wildland biomass fuels, J. Geophys.
763 Res.-Atmos., 118, 9914-9929, doi:10.1002/jgrd.50481, 2013.
764 Huang, R. J., Zhang, Y. L., Bozzetti, C., Ho, K. F., Cao, J. J., Han, Y. M., Daellenbach, K. R.,
765 Slowik, J. G., Platt, S. M., Canonaco, F., Zotter, P., Wolf, R., Pieber, S. M., Bruns, E. A.,
766 Crippa, M., Ciarelli, G., Piazzalunga, A., Schwikowski, M., Abbaszade, G., Schnelle-

767 Kreis, J., Zimmermann, R., An, Z. S., Szidat, S., Baltensperger, U., El Haddad, I., and
768 Prevot, A. S. H.: High secondary aerosol contribution to particulate pollution during haze
769 events in China, Nature, 514, 218-222, doi:10.1038/nature13774, 2014.
770 Huang, X., Ding, A., Liu, L., Liu, Q., Ding, K., Niu, X., Nie, W., Xu, Z., Chi, X., Wang, M.,
771 Sun, J., Guo, W., and Fu, C.: Effects of aerosol-radiation interaction on precipitation
772 during biomass-burning season in East China, Atmos. Chem. Phys., 16, 10063-10082,
773 doi:10.5194/acp-16-10063-2016, 2016.
774 Huang, Y., Shen, H. Z., Chen, Y. L., Zhong, Q. R., Chen, H., Wang, R., Shen, G. F., Liu, J. F.,
775 Li, B. G., and Tao, S.: Global organic carbon emissions from primary sources from 1960
776 to 2009, Atmos. Environ., 122, 505-512, doi:10.1016/j.atmosenv.2015.10.017, 2015.
777 Huang, Z., Zhang, Y., Yan, Q., Zhang, Z., and Wang, X.: Real-time monitoring of respiratory
778 absorption factors of volatile organic compounds in ambient air by proton transfer reaction
779 time-of-flight mass spectrometry, J. Hazard. Mater., 320, 547-555,
780 doi:10.1016/j.jhazmat.2016.08.064, 2016.
781 Huffman, J. A., Docherty, K. S., Mohr, C., Cubison, M. J., Ulbrich, I. M., Ziemann, P. J.,
782 Onasch, T. B., and Jimenez, J. L.: Chemically-resolved volatility measurements of organic
783 aerosol from different sources, Environ. Sci. Technol., 43, 5351-5357,
784 doi:10.1021/es803539d, 2009.
785 Jathar, S. H., Gordon, T. D., Hennigan, C. J., Pye, H. O. T., Pouliot, G., Adams, P. J., Donahue,
786 N. M., and Robinson, A. L.: Unspeciated organic emissions from combustion sources and
787 their influence on the secondary organic aerosol budget in the United States, Proc. Natl.
788 Acad. Sci. U. S. A., 111, 10473-10478, doi:10.1073/pnas.1323740111, 2014.
789 Jia, L., and Xu, Y.: Ozone and secondary organic aerosol formation from Ethylene-NO_x-NaCl
790 irradiations under different relative humidity conditions, J. Atmos. Chem., 73, 81-100,
791 doi:10.1007/s10874-015-9317-1, 2016.

792 Jolleys, M. D., Coe, H., McFiggans, G., Capes, G., Allan, J. D., Crosier, J., Williams, P. I.,
793 Allen, G., Bower, K. N., Jimenez, J. L., Russell, L. M., Grutter, M., and Baumgardner, D.:
794 Characterizing the aging of biomass burning organic aerosol by use of mixing ratios: a
795 meta-analysis of four regions, Environ. Sci. Technol., 46, 13093-13102,
796 doi:10.1021/es302386v, 2012.
797 Kim Oanh, N. T., Ly, B. T., Tipayarom, D., Manandhar, B. R., Prapat, P., Simpson, C. D., and
798 Sally Liu, L. J.: Characterization of particulate matter emission from open burning of rice
799 straw, Atmos. Environ., 45, 493-502, doi:10.1016/j.atmosenv.2010.09.023, 2011.
800 Kim Oanh, N. T., Tipayarom, A., Bich, T. L., Tipayarom, D., Simpson, C. D., Hardie, D., and
801 Sally Liu, L. J.: Characterization of gaseous and semi-volatile organic compounds emitted
802 from field burning of rice straw, Atmos. Environ., 119, 182-191,
803 doi:10.1016/j.atmosenv.2015.08.005, 2015.
804 Kirchstetter, T. W., and Novakov, T.: Controlled generation of black carbon particles from a
805 diffusion flame and applications in evaluating black carbon measurement methods, Atmos.
806 Environ., 41, 1874-1888, doi:10.1016/j.atmosenv.2006.10.067, 2007.
807 Koren, I., Kaufman, Y. J., Remer, L. A., and Martins, J. V.: Measurement of the effect of
808 Amazon smoke on inhibition of cloud formation, Science, 303, 1342-1345,
809 doi:10.1126/science.1089424, 2004.
810 Kroll, J. H., Donahue, N. M., Jimenez, J. L., Kessler, S. H., Canagaratna, M. R., Wilson, K. R.,
811 Altieri, K. E., Mazzoleni, L. R., Wozniak, A. S., and Bluhm, H.: Carbon oxidation state
812 as a metric for describing the chemistry of atmospheric organic aerosol, Nat. Chem., 3,
813 133-139, doi:10.1038/nchem.948, 2011.
814 Lambe, A. T., Ahern, A. T., Williams, L. R., Slowik, J. G., Wong, J. P. S., Abbatt, J. P. D.,
815 Brune, W. H., Ng, N. L., Wright, J. P., Croasdale, D. R., Worsnop, D. R., Davidovits, P.,
816 and Onasch, T. B.: Characterization of aerosol photooxidation flow reactors:

817 heterogeneous oxidation, secondary organic aerosol formation and cloud condensation
818 nuclei activity measurements, Atmos. Meas. Tech., 4, 445-461, doi:10.5194/amt-4-445-
819 2011, 2011.
820 Laskin, A., Laskin, J., and Nizkorodov, S. A.: Chemistry of atmospheric brown carbon, Chem.
821 Rev., 115, 4335-4382, doi:10.1021/cr5006167, 2015.
822 Li, C., Ma, Z., Chen, J., Wang, X., Ye, X., Wang, L., Yang, X., Kan, H., Donaldson, D. J., and
823 Mellouki, A.: Evolution of biomass burning smoke particles in the dark, Atmos. Environ.,
824 120, 244-252, doi:10.1016/j.atmosenv.2015.09.003, 2015.
825 Li, C., Hu, Y., Zhang, F., Chen, J., Ma, Z., Ye, X., Yang, X., Wang, L., Tang, X., Zhang, R., Mu,
826 M., Wang, G., Kan, H., Wang, X., and Mellouki, A.: Multi-pollutant emissions from the
827 burning of major agricultural residues in China and the related health-economic effects,
828 Atmos. Chem. Phys., 17, 4957-4988, doi:10.5194/acp-17-4957-2017, 2017.
829 Li, J., Bo, Y., and Xie, S. D.: Estimating emissions from crop residue open burning in China
830 based on statistics and MODIS fire products, J. Environ. Sci., 44, 158-170,
831 doi:10.1016/j.jes.2015.08.024, 2016.
832 Li, Q., Li, X. H., Jiang, J. K., Duan, L., Ge, S., Zhang, Q., Deng, J. G., Wang, S. X., and Hao,
833 J. M.: Semi-coke briquettes: towards reducing emissions of primary $PM_{2.5}$, particulate
834 carbon, and carbon monoxide from household coal combustion in China, Sci. Rep., 6, 10,
835 doi:10.1038/srep19306, 2016.
836 Li, X. G., Wang, S. X., Duan, L., Hao, J., Li, C., Chen, Y. S., and Yang, L.: Particulate and trace
837 gas emissions from open burning of wheat straw and corn stover in China, Environ. Sci.
838 Technol., 41, 6052-6058, doi:10.1021/es0705137, 2007.
839 Li, X. H., Wang, S. X., Duan, L., and Hao, J. M.: Characterization of non-methane
840 hydrocarbons emitted from open burning of wheat straw and corn stover in China, Environ.
841 Res. Lett., 4, 7, doi:10.1088/1748-9326/4/4/044015, 2009.

842 Lim, Y. B., Tan, Y., and Turpin, B. J.: Chemical insights, explicit chemistry, and yields of
843 secondary organic aerosol from OH radical oxidation of methylglyoxal and glyoxal in the
844 aqueous phase, Atmos. Chem. Phys., 13, 8651-8667, doi:10.5194/acp-13-8651-2013,
845 2013.
846 Lipsky, E. M., and Robinson, A. L.: Effects of dilution on fine particle mass and partitioning
847 of semivolatile organics in diesel exhaust and wood smoke, Environ. Sci. Technol., 40,
848 155-162, doi:10.1021/es050319p, 2006.
849 Liu, C., Zhang, C., Mu, Y., Liu, J., and Zhang, Y.: Emission of volatile organic compounds
850 from domestic coal stove with the actual alternation of flaming and smoldering
851 combustion processes, Environ. Pollut., 221, 385-391, doi:10.1016/j.envpol.2016.11.089,
852 2017.
853 Liu, J., Mauzerall, D. L., Chen, Q., Zhang, Q., Song, Y., Peng, W., Klimont, Z., Qiu, X., Zhang,
854 S., Hu, M., Lin, W., Smith, K. R., and Zhu, T.: Air pollutant emissions from Chinese
855 households: A major and underappreciated ambient pollution source, Proc. Natl. Acad.
856 Sci., doi:10.1073/pnas.1604537113, 2016.
857 Liu, T., Wang, X., Deng, W., Hu, Q., Ding, X., Zhang, Y., He, Q., Zhang, Z., Lu, S., Bi, X.,
858 Chen, J., and Yu, J.: Secondary organic aerosol formation from photochemical aging of
859 light-duty gasoline vehicle exhausts in a smog chamber, Atmos. Chem. Phys., 15, 9049-
860 9062, doi:10.5194/acp-15-9049-2015, 2015.
861 Liu, X. X., Zhang, Y., Huey, L. G., Yokelson, R. J., Wang, Y., Jimenez, J. L., Campuzano-Jost,
862 P., Beyersdorf, A. J., Blake, D. R., Choi, Y., St Clair, J. M., Crounse, J. D., Day, D. A.,
863 Diskin, G. S., Fried, A., Hall, S. R., Hanisco, T. F., King, L. E., Meinardi, S., Mikoviny,
864 T., Palm, B. B., Peischl, J., Perring, A. E., Pollack, I. B., Ryerson, T. B., Sachse, G.,
865 Schwarz, J. P., Simpson, I. J., Tanner, D. J., Thornhill, K. L., Ullmann, K., Weber, R. J.,
866 Wennberg, P. O., Wisthaler, A., Wolfe, G. M., and Ziemba, L. D.: Agricultural fires in the

867 southeastern US during SEAC[4]RS: Emissions of trace gases and particles and evolution
868 of ozone, reactive nitrogen, and organic aerosol, J. Geophys. Res.-Atmos., 121, 7383-
869 7414, doi:10.1002/2016jd025040, 2016.
870 Martin, M., Tritscher, T., Juranyi, Z., Heringa, M. F., Sierau, B., Weingartner, E., Chirico, R.,
871 Gysel, M., Prevot, A. S. H., Baltensperger, U., and Lohmann, U.: Hygroscopic properties
872 of fresh and aged wood burning particles, J. Aerosol Sci., 56, 15-29,
873 doi:10.1016/j.jaerosci.2012.08.006, 2013.
874 May, A. A., Levin, E. J. T., Hennigan, C. J., Riipinen, I., Lee, T., Collett, J. L., Jr., Jimenez, J.
875 L., Kreidenweis, S. M., and Robinson, A. L.: Gas-particle partitioning of primary organic
876 aerosol emissions: 3. Biomass burning, J. Geophys. Res.-Atmos., 118, 11327-11338,
877 doi:10.1002/jgrd.50828, 2013.
878 May, A. A., Lee, T., McMeeking, G. R., Akagi, S., Sullivan, A. P., Urbanski, S., Yokelson, R.
879 J., and Kreidenweis, S. M.: Observations and analysis of organic aerosol evolution in some
880 prescribed fire smoke plumes, Atmos. Chem. Phys., 15, 6323-6335, doi:10.5194/acp-15-
881 6323-2015, 2015.
882 McMurry, P. H., and Grosjean, D.: Gas and aerosol wall losses in Teflon film smog chambers,
883 Environ. Sci. Technol., 19, 1176-1182, doi:10.1021/es00142a006, 1985.
884 Müller, M., Anderson, B. E., Beyersdorf, A. J., Crawford, J. H., Diskin, G. S., Eichler, P., Fried,
885 A., Keutsch, F. N., Mikoviny, T., Thornhill, K. L., Walega, J. G., Weinheimer, A. J., Yang,
886 M., Yokelson, R. J., and Wisthaler, A.: In situ measurements and modeling of reactive
887 trace gases in a small biomass burning plume, Atmos. Chem. Phys., 16, 3813-3824,
888 doi:10.5194/acp-16-3813-2016, 2016.
889 Nakao, S., Clark, C., Tang, P., Sato, K., and Iii, D. C.: Secondary organic aerosol formation
890 from phenolic compounds in the absence of NO_x, Atmos. Chem. Phys., 11, 2025-2055,
891 doi:10.5194/acp-11-10649-2011, 2011.

National bureau of statistics of people's republic of China.: China Energy Statistical Yearbook 2013, China Stat. Press, Beijing, 2014.

National bureau of statistics of people's republic of China.: The statistical communiqu on national economy and social development in 2015, http://www.stats.gov.cn/tjsj/zxfb/201602/t20160229_1323991.html, last accessed: 27 September 2017.

Ng, N. L., Chhabra, P. S., Chan, A. W. H., Surratt, J. D., Kroll, J. H., Kwan, A. J., McCabe, D. C., Wennberg, P. O., Sorooshian, A., Murphy, S. M., Dalleska, N. F., Flagan, R. C., and Seinfeld, J. H.: Effect of NO_x level on secondary organic aerosol (SOA) formation from the photooxidation of terpenes, Atmos. Chem. Phys., 7, 5159-5174, doi:10.5194/acp-7-5159-2007, 2007a.

Ng, N. L., Kroll, J. H., Chan, A. W. H., Chhabra, P. S., Flagan, R. C., and Seinfeld, J. H.: Secondary organic aerosol formation from m-xylene, toluene, and benzene, Atmos. Chem. Phys., 7, 3909-3922, doi:10.5194/acp-7-3909-2007, 2007b.

Ng, N. L., Canagaratna, M. R., Zhang, Q., Jimenez, J. L., Tian, J., Ulbrich, I. M., Kroll, J. H., Docherty, K. S., Chhabra, P. S., Bahreini, R., Murphy, S. M., Seinfeld, J. H., Hildebrandt, L., Donahue, N. M., DeCarlo, P. F., Lanz, V. A., Prevot, A. S. H., Dinar, E., Rudich, Y., and Worsnop, D. R.: Organic aerosol components observed in Northern Hemispheric datasets from Aerosol Mass Spectrometry, Atmos. Chem. Phys., 10, 4625-4641, doi:10.5194/acp-10-4625-2010, 2010.

Ng, N. L., Canagaratna, M. R., Jimenez, J. L., Chhabra, P. S., Seinfeld, J. H., and Worsnop, D. R.: Changes in organic aerosol composition with aging inferred from aerosol mass spectra, Atmos. Chem. Phys., 11, 6465-6474, doi:10.5194/acp-11-6465-2011, 2011a.

Ng, N. L., Canagaratna, M. R., Jimenez, J. L., Zhang, Q., Ulbrich, I. M., and Worsnop, D. R.: Real-Time Methods for estimating organic cComponent mass concentrations from aerosol

mass spectrometer data, Environ. Sci. Technol., 45, 910-916, doi:10.1021/es102951k, 2011b.

Ni, H. Y., Han, Y. M., Cao, J. J., Chen, L. W. A., Tian, J., Wang, X. L., Chow, J. C., Watson, J. G., Wang, Q. Y., Wang, P., Li, H., and Huang, R. J.: Emission characteristics of carbonaceous particles and trace gases from open burning of crop residues in China, Atmos. Environ., 123, 399-406, doi:10.1016/j.atmosenv.2015.05.007, 2015.

Niu, H. Y., Cheng, W. J., Hu, W., and Pian, W.: Characteristics of individual particles in a severe short-period haze episode induced by biomass burning in Beijing, Atmos. Pollut. Res., 7, 1072-1081, doi:10.1016/j.apr.2016.05.011, 2016.

Ortega, A. M., Day, D. A., Cubison, M. J., Brune, W. H., Bon, D., de Gouw, J. A., and Jimenez, J. L.: Secondary organic aerosol formation and primary organic aerosol oxidation from biomass-burning smoke in a flow reactor during FLAME-3, Atmos. Chem. Phys., 13, 11551-11571, doi:10.5194/acp-13-11551-2013, 2013.

Pan, X., Kanaya, Y., Tanimoto, H., Inomata, S., Wang, Z., Kudo, S., and Uno, I.: Examining the major contributors of ozone pollution in a rural area of the Yangtze River Delta region during harvest season, Atmos. Chem. Phys., 15, 6101-6111, doi:10.5194/acp-15-6101-2015, 2015.

Presto, A. A., Miracolo, M. A., Kroll, J. H., Worsnop, D. R., Robinson, A. L., and Donahue, N. M.: Intermediate-volatility organic compounds: A potential source of ambient oxidized organic aerosol, Environ. Sci. Technol., 43, 4744-4749, doi:10.1021/es803219q, 2009.

Real, E., Law, K. S., Weinzierl, B., Fiebig, M., Petzold, A., Wild, O., Methven, J., Arnold, S., Stohl, A., Huntrieser, H., Roiger, A., Schlager, H., Stewart, D., Avery, M., Sachse, G., Browell, E., Ferrare, R., and Blake, D.: Processes influencing ozone levels in Alaskan forest fire plumes during long-range transport over the North Atlantic, J. Geophys. Res.-Atmos., 112, doi:10.1029/2006jd007576, 2007.

Robinson, A. L., Donahue, N. M., Shrivastava, M. K., Weitkamp, E. A., Sage, A. M., Grieshop, A. P., Lane, T. E., Pierce, J. R., and Pandis, S. N.: Rethinking organic aerosols: semivolatile emissions and photochemical aging, Science, 315, 1259-1262, doi:10.1126/science.1133061, 2007.

Sanchis, E., Ferrer, M., Calvet, S., Coscolla, C., Yusa, V., and Cambra-Lopez, M.: Gaseous and particulate emission profiles during controlled rice straw burning, Atmos. Environ., 98, 25-31, doi:10.1016/j.atmosenv.2014.07.062, 2014.

Schmid, O., Artaxo, P., Arnott, W. P., Chand, D., Gatti, L. V., Frank, G. P., Hoffer, A., Schnaiter, M., and Andreae, M. O.: Spectral light absorption by ambient aerosols influenced by biomass burning in the Amazon Basin. I: Comparison and field calibration of absorption measurement techniques, Atmos. Chem. Phys., 6, 3443-3462, doi:10.5194/acp-6-3443-2006, 2006.

Schmid, O., Karg, E., Hagen, D. E., Whitefield, P. D., and Ferron, G. A.: On the effective density of non-spherical particles as derived from combined measurements of aerodynamic and mobility equivalent size, J. Aerosol Sci., 38, 431-443, doi:10.1016/j.jaerosci.2007.01.002, 2007.

Shahid, I., Kistler, M., Mukhtar, A., Cruz, C. R. S., Bauer, H., and Puxbaum, H.: Chemical composition of particles from traditional burning of Pakistani wood species, Atmos. Environ., 121, 35-41, doi:10.1016/j.atmosenv.2015.01.041, 2015.

Shakya, K. M., and Griffin, R. J.: Secondary organic aerosol from photooxidation of polycyclic aromatic hydrocarbons, Environ. Sci. Technol., 44, 8134-8139, doi:10.1021/es1019417, 2010.

Shrivastava, M., Easter, R. C., Liu, X. H., Zelenyuk, A., Singh, B., Zhang, K., Ma, P. L., Chand, D., Ghan, S., Jimenez, J. L., Zhang, Q., Fast, J., Rasch, P. J., and Tiitta, P.: Global transformation and fate of SOA: Implications of low-volatility SOA and gas-phase

967 fragmentation reactions, J. Geophys. Res.-Atmos., 120, 4169-4195,
968 doi:10.1002/2014jd022563, 2015.
969 Spracklen, D. V., Jimenez, J. L., Carslaw, K. S., Worsnop, D. R., Evans, M. J., Mann, G. W.,
970 Zhang, Q., Canagaratna, M. R., Allan, J., Coe, H., McFiggans, G., Rap, A., and Forster,
971 P.: Aerosol mass spectrometer constraint on the global secondary organic aerosol budget,
972 Atmos. Chem. Phys., 11, 12109-12136, doi:10.5194/acp-11-12109-2011, 2011.
973 Stockwell, C. E., Yokelson, R. J., Kreidenweis, S. M., Robinson, A. L., DeMott, P. J., Sullivan,
974 R. C., Reardon, J., Ryan, K. C., Griffith, D. W. T., and Stevens, L.: Trace gas emissions
975 from combustion of peat, crop residue, domestic biofuels, grasses, and other fuels:
976 configuration and Fourier transform infrared (FTIR) component of the fourth Fire Lab at
977 Missoula Experiment (FLAME-4), Atmos. Chem. Phys., 14, 9727-9754,
978 doi:10.5194/acp-14-9727-2014, 2014.
979 Stockwell, C. E., Veres, P. R., Williams, J., and Yokelson, R. J.: Characterization of biomass
980 burning emissions from cooking fires, peat, crop residue, and other fuels with high-
981 resolution proton-transfer-reaction time-of-flight mass spectrometry, Atmos. Chem. Phys.,
982 15, 845-865, doi:10.5194/acp-15-845-2015, 2015.
983 Stockwell, C. E., Christian, T. J., Goetz, J. D., Jayarathne, T., Bhave, P. V., Praveen, P. S.,
984 Adhikari, S., Maharjan, R., DeCarlo, P. F., Stone, E. A., Saikawa, E., Blake, D. R.,
985 Simpson, I. J., Yokelson, R. J., and Panday, A. K.: Nepal Ambient Monitoring and Source
986 Testing Experiment (NAMaSTE): emissions of trace gases and light-absorbing carbon
987 from wood and dung cooking fires, garbage and crop residue burning, brick kilns, and
988 other sources, Atmos. Chem. Phys., 16, 11043-11081, 10.5194/acp-16-11043-2016, 2016.
989 Streets, D. G., Yarber, K. F., Woo, J. H., and Carmichael, G. R.: Biomass burning in Asia:
990 Annual and seasonal estimates and atmospheric emissions, Global Biogeochem. Cy., 17,
991 20, doi:10.1029/2003gb002040, 2003.

992 Takekawa, H., Minoura, H., and Yamazaki, S.: Temperature dependence of secondary organic
993 aerosol formation by photo-oxidation of hydrocarbons, Atmos. Environ., 37, 3413-3424,
994 doi:10.1016/s1352-2310(03)00359-5, 2003.
995 Tariq, S., ul-Haq, Z., and Ali, M.: Satellite and ground-based remote sensing of aerosols during
996 intense haze event of October 2013 over lahore, Pakistan, Asia-Pac. J. Atmos. Sci., 52,
997 25-33, doi:10.1007/s13143-015-0084-3, 2016.
998 Tkacik, D. S., Robinson, E. S., Ahern, A., Saleh, R., Stockwell, C., Veres, P., Simpson, I. J.,
999 Meinardi, S., Blake, D. R., Yokelson, R. J., Presto, A. A., Sullivan, R. C., Donahue, N. M.,
1000 and Robinson, A. L.: A dual-chamber method for quantifying the effects of atmospheric
1001 perturbations on secondary organic aerosol formation from biomass burning emissions, J.
1002 Geophys. Res.-Atmos., 122, 6043-6058, doi:10.1002/2016JD025784, 2017.
1003 Thompson, A. M., Witte, J. C., Hudson, R. D., Guo, H., Herman, J. R., and Fujiwara, M.:
1004 Tropical tropospheric ozone and biomass burning, Science, 291, 2128-2132,
1005 doi:10.1126/science.291.5511.2128, 2001.
1006 Tian, H., Zhao, D., and Wang, Y.: Emission inventories of atmospheric pollutants discharged
1007 from biomass burning in China, Acta Sci. Circumst., 31, 349-357 in Chinese, 2011.
1008 Tissari, J., Lyyranen, J., Hytonen, K., Sippula, O., Tapper, U., Frey, A., Saarnio, K., Pennanen,
1009 A. S., Hillamo, R., Salonen, R. O., Hirvonen, M. R., and Jokiniemi, J.: Fine particle and
1010 gaseous emissions from normal and smouldering wood combustion in a conventional
1011 masonry heater, Atmos. Environ., 42, 7862-7873, doi:10.1016/j.atmosenv.2008.07.019,
1012 2008.
1013 Tiitta, P., Leskinen, A., Hao, L., Yli-Pirila, P., Kortelainen, M., Grigonyte, J., Tissari, J.,
1014 Lamberg, H., Hartikainen, A., Kuuspalo, K., Kortelainen, A.-M., Virtanen, A., Lehtinen,
1015 K. E. J., Komppula, M., Pieber, S., Prevot, A. S. H., Onasch, T. B., Worsnop, D. R., Czech,
1016 H., Zimmermann, R., Jokiniemi, J., and Sippula, O.: Transformation of logwood

combustion emissions in a smog chamber: formation of secondary organic aerosol and changes in the primary organic aerosol upon daytime and nighttime aging, Atmos. Chem. Phys., 16, 13251-13269, doi:10.5194/acp-16-13251-2016, 2016.

Tsigaridis, K., Daskalakis, N., Kanakidou, M., Adams, P. J., Artaxo, P., Bahadur, R., Balkanski, Y., Bauer, S. E., Bellouin, N., Benedetti, A., Bergman, T., Berntsen, T. K., Beukes, J. P., Bian, H., Carslaw, K. S., Chin, M., Curci, G., Diehl, T., Easter, R. C., Ghan, S. J., Gong, S. L., Hodzic, A., Hoyle, C. R., Iversen, T., Jathar, S., Jimenez, J. L., Kaiser, J. W., Kirkevåg, A., Koch, D., Kokkola, H., Lee, Y. H., Lin, G., Liu, X., Luo, G., Ma, X., Mann, G. W., Mihalopoulos, N., Morcrette, J. J., Müller, J. F., Myhre, G., Myriokefalitakis, S., Ng, N. L., O'Donnell, D., Penner, J. E., Pozzoli, L., Pringle, K. J., Russell, L. M., Schulz, M., Sciare, J., Seland, Ø., Shindell, D. T., Sillman, S., Skeie, R. B., Spracklen, D., Stavrakou, T., Steenrod, S. D., Takemura, T., Tiitta, P., Tilmes, S., Tost, H., van Noije, T., van Zyl, P. G., von Salzen, K., Yu, F., Wang, Z., Wang, Z., Zaveri, R. A., Zhang, H., Zhang, K., Zhang, Q., and Zhang, X.: The AeroCom evaluation and intercomparison of organic aerosol in global models, Atmos. Chem. Phys., 14, 10845-10895, doi:10.5194/acp-14-10845-2014, 2014.

Wang, H., Lou, S., Huang, C., Qiao, L., Tang, X., Chen, C., Zeng, L., Wang, Q., Zhou, M., Lu, S., and Yu, X.: Source profiles of volatile organic compounds from biomass burning in Yangtze River Delta, China, Aerosol Air Qual. Res., 14, 818-828, doi:10.4209/aaqr.2013.05.0174, 2014.

Wang, X., and Wu, T.: Release of isoprene and monoterpenes during the aerobic decomposition of orange wastes from laboratory incubation experiments, Environ. Sci. Technol., 42, 3265-3270, doi:10.1021/es702999j, 2008.

Wang, X., Liu, T., Bernard, F., Ding, X., Wen, S., Zhang, Y., Zhang, Z., He, Q., Lu, S., Chen, J., Saunders, S., and Yu, J.: Design and characterization of a smog chamber for studying

gas-phase chemical mechanisms and aerosol formation, Atmos. Meas. Tech., 7, 301-313, doi:10.5194/amt-7-301-2014, 2014.

Ward, D. E., Susott, R. A., Kauffman, J. B., Babbitt, R. E., Cummings, D. L., Dias, B., Holben, B. N., Kaufman, Y. J., Rasmussen, R. A., and Setzer, A. W.: Smoke and fire characteristics for cerrado and deforestation burns in Brazil: BASE-B Experiment, J. Geophys. Res.-Atmos., 97, 14601-14619, doi:10.1029/92JD01218, 1992.

Weimer, S., Alfarra, M. R., Schreiber, D., Mohr, M., Prevot, A. S. H., and Baltensperger, U.: Organic aerosol mass spectral signatures from wood-burning emissions: Influence of burning conditions and wood type, J. Geophys. Res.-Atmos., 113, doi:10.1029/2007jd009309, 2008.

Weitkamp, E. A., Sage, A. M., Pierce, J. R., Donahue, N. M., and Robinson, A. L.: Organic aerosol formation from photochemical oxidation of diesel exhaust in a smog chamber, Environ. Sci. Technol., 41, 6969-6975, doi:10.1021/es070193r, 2007.

Yee, L. D., Kautzman, K. E., Loza, C. L., Schilling, K. A., Coggon, M. M., Chhabra, P. S., Chan, M. N., Chan, A. W. H., Hersey, S. P., Crounse, J. D., Wennberg, P. O., Flagan, R. C., and Seinfeld, J. H.: Secondary organic aerosol formation from biomass burning intermediates: phenol and methoxyphenols, Atmos. Chem. Phys., 13, 8019-8043, doi:10.5194/acp-13-8019-2013, 2013.

Yi, Z. G., Wang, X. M., Sheng, G. Y., Zhang, D. Q., Zhou, G. Y., and Fu, J. M.: Soil uptake of carbonyl sulfide in subtropical forests with different successional stages in south China, J. Geophys. Res.-Atmos., 112, 11, doi:10.1029/2006jd008048, 2007.

Yokelson, R. J., Christian, T. J., Karl, T. G., and Guenther, A.: The tropical forest and fire emissions experiment: laboratory fire measurements and synthesis of campaign data, Atmos. Chem. Phys., 8, 3509-3527, doi:10.5194/acp-8-3509-2008, 2008.

Yokelson, R. J., Burling, I. R., Urbanski, S. P., Atlas, E. L., Adachi, K., Buseck, P. R.,

1067 Wiedinmyer, C., Akagi, S. K., Toohey, D. W., and Wold, C. E.: Trace gas and particle
1068 emissions from open biomass burning in Mexico, Atmos. Chem. Phys., 11, 6787-6808,
1069 doi:10.5194/acp-11-6787-2011, 2011.
1070 Zhang, H., Ye, X., Cheng, T., Chen, J., Yang, X., Wang, L., and Zhang, R.: A laboratory study
1071 of agricultural crop residue combustion in China: Emission factors and emission inventory,
1072 Atmos. Environ., 42, 8432-8441, doi:10.1016/j.atmosenv.2008.08.015, 2008.
1073 Zhang, H., Hu, D., Chen, J., Ye, X., Wang, S. X., Hao, J. M., Wang, L., Zhang, R., and An, Z.:
1074 Particle size distribution and polycyclic aromatic hydrocarbons emissions from
1075 agricultural crop residue burning, Environ. Sci. Technol., 45, 5477-5482,
1076 doi:10.1021/es1037904, 2011.
1077 Zhang, Q., Jimenez, J.L., Canagaratna, M.R., Ulbrich, I.M., Ng, N.L., Worsnop, D.R., Sun,
1078 Y.L.: Understanding atmospheric organic aerosols via factor analysis of aerosol mass
1079 spectrometry: a review, Anal. Bioanal. Chem., 401, 3045-3067, doi: 10.1007/s00216-011-
1080 5355-y, 2011
1081 Zhang, Y. L., Guo, H., Wang, X. M., Simpson, I. J., Barletta, B., Blake, D. R., Meinardi, S.,
1082 Rowland, F. S., Cheng, H. R., Saunders, S. M., and Lam, S. H. M.: Emission patterns and
1083 spatiotemporal variations of halocarbons in the Pearl River Delta region, southern China,
1084 J. Geophys. Res.-Atmos., 115, 16, doi:10.1029/2009jd013726, 2010.
1085 Zhang, Y. L., Wang, X. M., Blake, D. R., Li, L. F., Zhang, Z., Wang, S. Y., Guo, H., Lee, F. S.
1086 C., Gao, B., Chan, L. Y., Wu, D., and Rowland, F. S.: Aromatic hydrocarbons as ozone
1087 precursors before and after outbreak of the 2008 financial crisis in the Pearl River Delta
1088 region, south China, J. Geophys. Res.-Atmos., 117, 16, doi:10.1029/2011jd017356, 2012.
1089 Zhao, Y. L., Hennigan, C. J., May, A. A., Tkacik, D. S., de Gouw, J. A., Gilman, J. B., Kuster,
1090 W. C., Borbon, A., and Robinson, A. L.: Intermediate-volatility organic compounds: A
1091 large source of secondary organic aerosol, Environ. Sci. Technol., 48, 13743-13750,

doi:10.1021/es5035188, 2014.

Zhu, Y. H., Yang, L. X., Chen, J. M., Wang, X. F., Xue, L. K., Sui, X., Wen, L., Xu, C. H., Yao, L., Zhang, J. M., Shao, M., Lu, S. H., and Wang, W. X.: Characteristics of ambient volatile organic compounds and the influence of biomass burning at a rural site in Northern China during summer 2013, Atmos. Environ., 124, 156-165, doi:10.1016/j.atmosenv.2015.08.097, 2016.

Table 1. Primary emission factors measured for agricultural residues burning. All the units are g kg^{-1}, except the unit for particle number (PN) is 10^{15} particle kg^{-1}. MCE: modified combustion efficiency; NMHCs: non-methane hydrocarbons; POA: primary organic aerosol; POC primary organic carbon; BC: black carbon.

	Rice		Corn		Wheat	
Species	This study (n=9)	Others	This study (n=6)	Others	This study (n=5)	Others
MCE	0.926±0.049		0.953±0.019		0.949±0.035	
CO_2	1262±81		1477±28		1423±60	
CO	63.5±41.4		46.1±19.2		48.6±33.0	
NO_x	1.47±0.61	3.51±0.38[a]	5.00±3.94	4.3±1.8[b]	3.08±0.93	3.3±1.7[b]; 2.27±0.04[a]
NH_3	0.45±0.15	0.95±0.65[a]; 4.10±1.24[c]	0.63±0.30	0.68±0.52[b]	0.22±0.19	0.37±0.14[b]; 0.21±0.14[a]
SO_2	0.07±0.07	0.18±0.31[d]; 0.37±0.27[e]; 1.27±0.35[a]	0.99±1.53	0.04±0.04[d]	0.72±0.34	0.04±0.04[d]; 0.73±0.15[a]
NMHCs	5.04±2.04	1.25[f]	2.47±2.11	1.59±0.43[g]	3.08±2.43	1.69±0.58[g]; 0.90[f]
PM	3.73±3.28	8.5±6.7[h]; 8.3±2.2[e]; 13.2±1.44[i]; 4.2[c]	5.44±3.43	12.2±5.4[h]; 11.7±1.0[b]; 5.36±0.55[i]	6.36±2.98	11.4±4.9[h]; 7.6±4.1[b]; 5.30±0.30[i]
PN	2.94±0.91	0.018±0.001[j]	7.29±4.17	0.017±0.001[j]	5.87±2.89	0.010±0.001[j]
POA	2.99±1.00		3.99±2.68		5.96±0.19	
POC	2.05±0.72	3.3±2.8[h]; 6.02±0.60[i]	2.52±1.66	6.3±3.6[h]; 3.9±1.7[b]; 2.06±0.34[i]	4.11±0.29	5.1±3.0[h]; 2.7±1.0[b]; 2.42±0.13[i]
BC	0.22±0.11	0.21±0.13[h]	0.24±0.09	0.28±0.09[h]; 0.35±0.10[b]	0.27±0.07	0.24±0.12[h]; 0.49±0.12[b]

[a] Stockwell et al., 2015; [b] Li et al., 2007, PM correspond to $PM_{2.5}$; [c] Christian et al., 2003; [d] Cao et al., 2008; [e] Kim Oanh et al., 2015, PM correspond to $PM_{2.5}$; [f] Wang et al., 2014, 56 NMHCs species summarized; [g] Li et al., 2009, 52 NMHCs species summarized; [h] Ni et al., 2015, PM correspond to $PM_{2.5}$; [i] Li et al., 2017, PM correspond to PM_1; [j] Zhang et al., 2008.

Table 2. Overview of important experimental conditions and key results in the photochemical oxidation experiments. The unit for OH exposure is 10^{10} molecule cm^{-3} s. NA: data was not available because no data was recorded in the W-mode.

NO.	Straw type	Temp (°C)	RH (%)	OH exposure	POA			Aged OA			OA ER
					O/C	H/C	OS_c	O/C	H/C	OS_c	
Burn 1	Rice	25.0±0.4	48.9±1.4	3.80	NA	NA	NA	NA	NA	NA	2.7
Burn 2	Rice	25.1±0.4	55.0±2.3	4.97	0.25	1.74	-1.25	0.50	1.65	-0.65	7.6
Burn 3	Corn	25.5±0.4	53.0±2.9	4.16	0.38	1.66	-0.89	0.60	1.66	-0.46	3.6
Burn 4	Corn	26.1±0.4	48.4±2.2	4.16	0.30	1.58	-0.97	0.65	1.57	-0.26	4.6
Burn 5	Wheat	25.3±0.5	52.8±2.2	3.20	0.20	1.66	-1.25	0.50	1.56	-0.55	2.4
Burn 6	Wheat	25.2±0.4	55.1±2.7	1.87	0.26	1.71	-1.20	0.53	1.66	-0.61	6.6

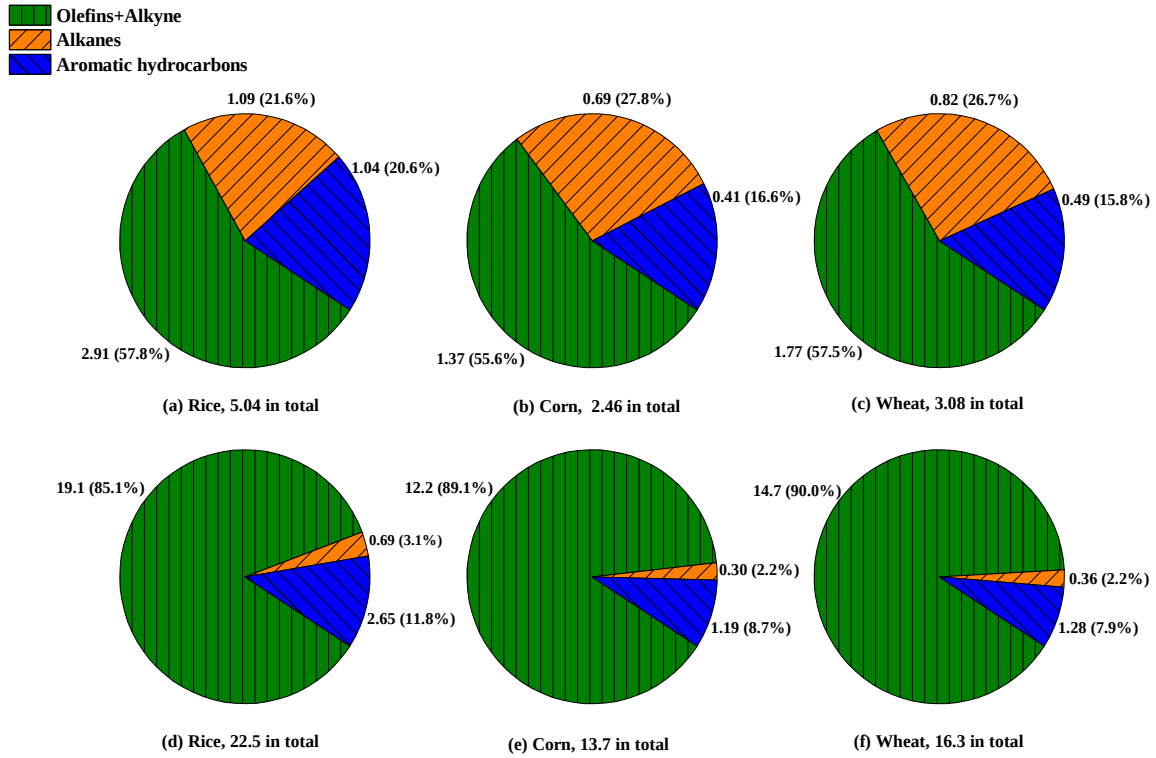

Figure 1. (a-c) Non-methane hydrocarbon (NMHC) compositions and (d-f) their relative contribution to ozone formation potential (OFP) for open burning of rice, corn and wheat straw.

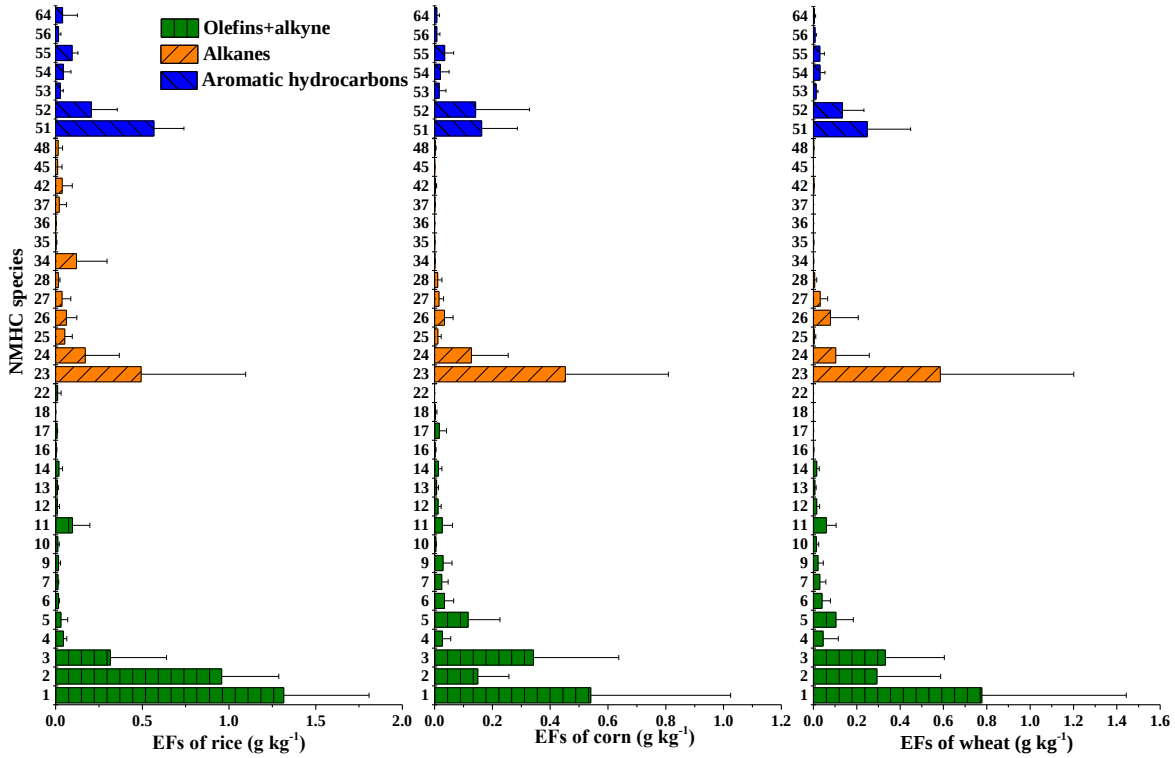

Figure 2. Emission factors (EFs) of NMHCs for straw burning of rice, corn and wheat. Only species with emission factors >0.01 g kg^{-1} are shown. The order of NMHC species is the same as Table S1 in which a comprehensive dataset of emission factors measured in this work is included.

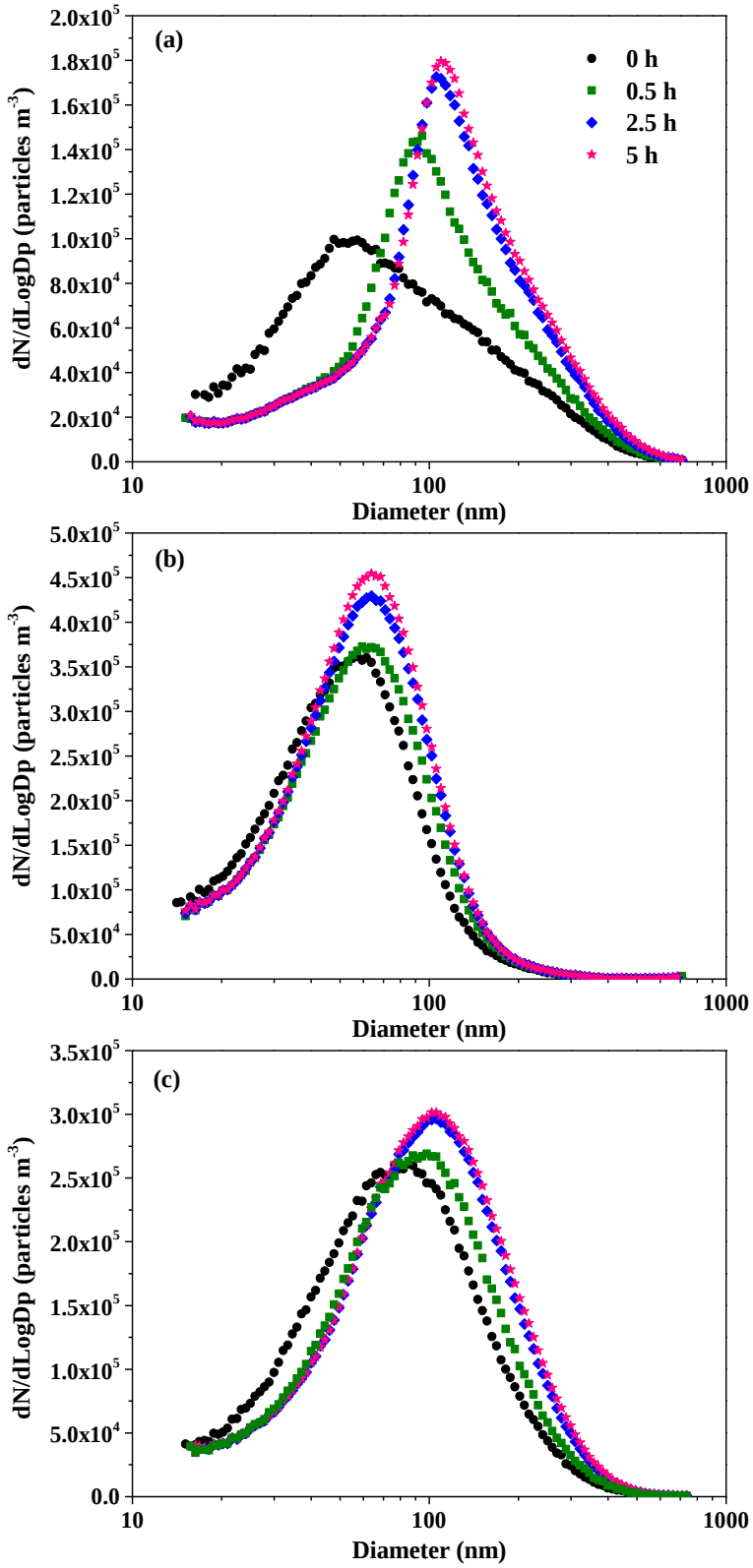

1124

1125 **Figure 3.** Particle size distributions in different burning. (a) Burn 2: rice straw; (b) Burn 3:

1126 corn straw, (c) Burn 5: wheat straw.

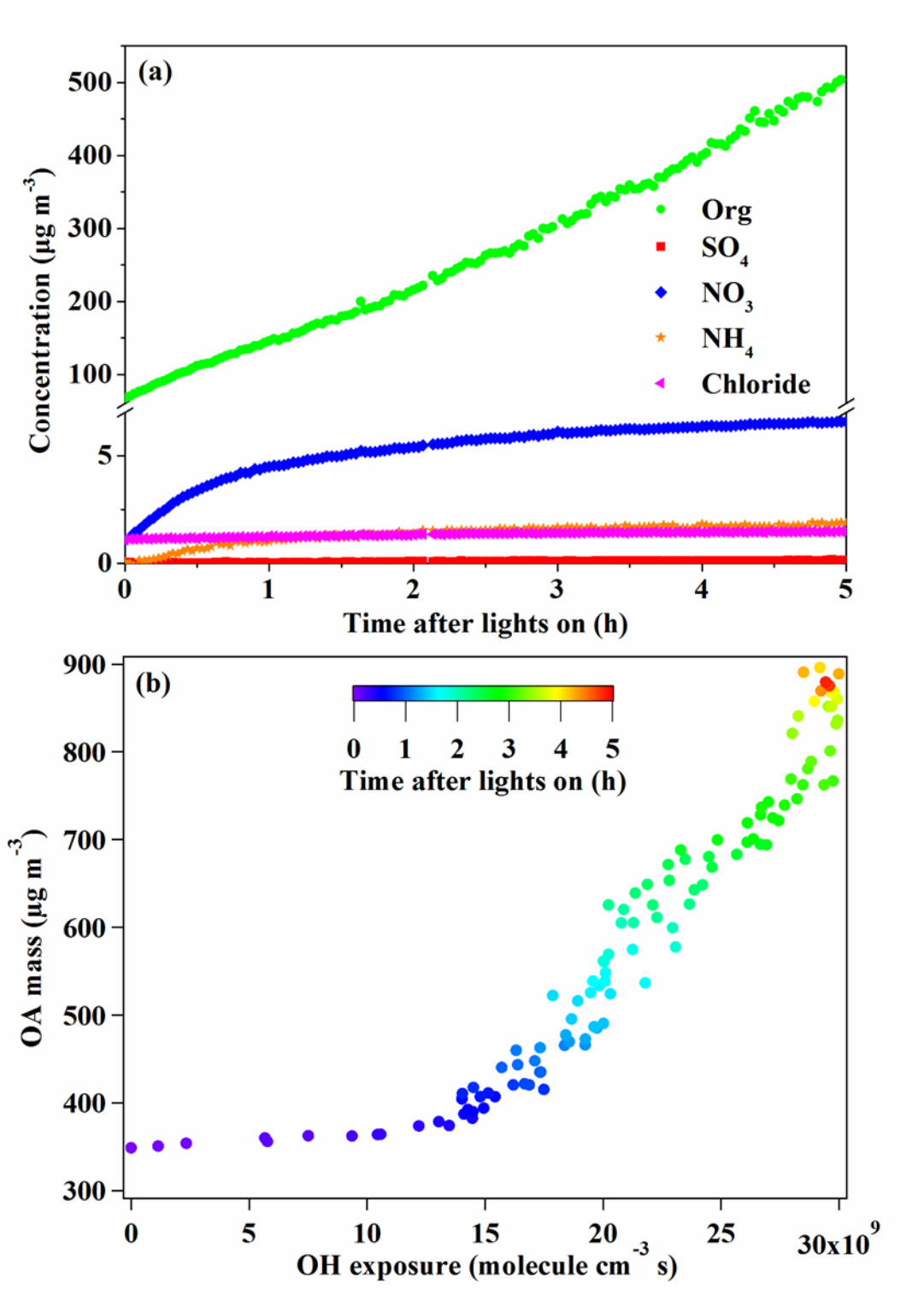

1127

1128 **Figure 4.** (a) The evolution of particulate matter components (Burn 2). (b) OA mass growth as

1129 a function of OH exposure (Burn 5).

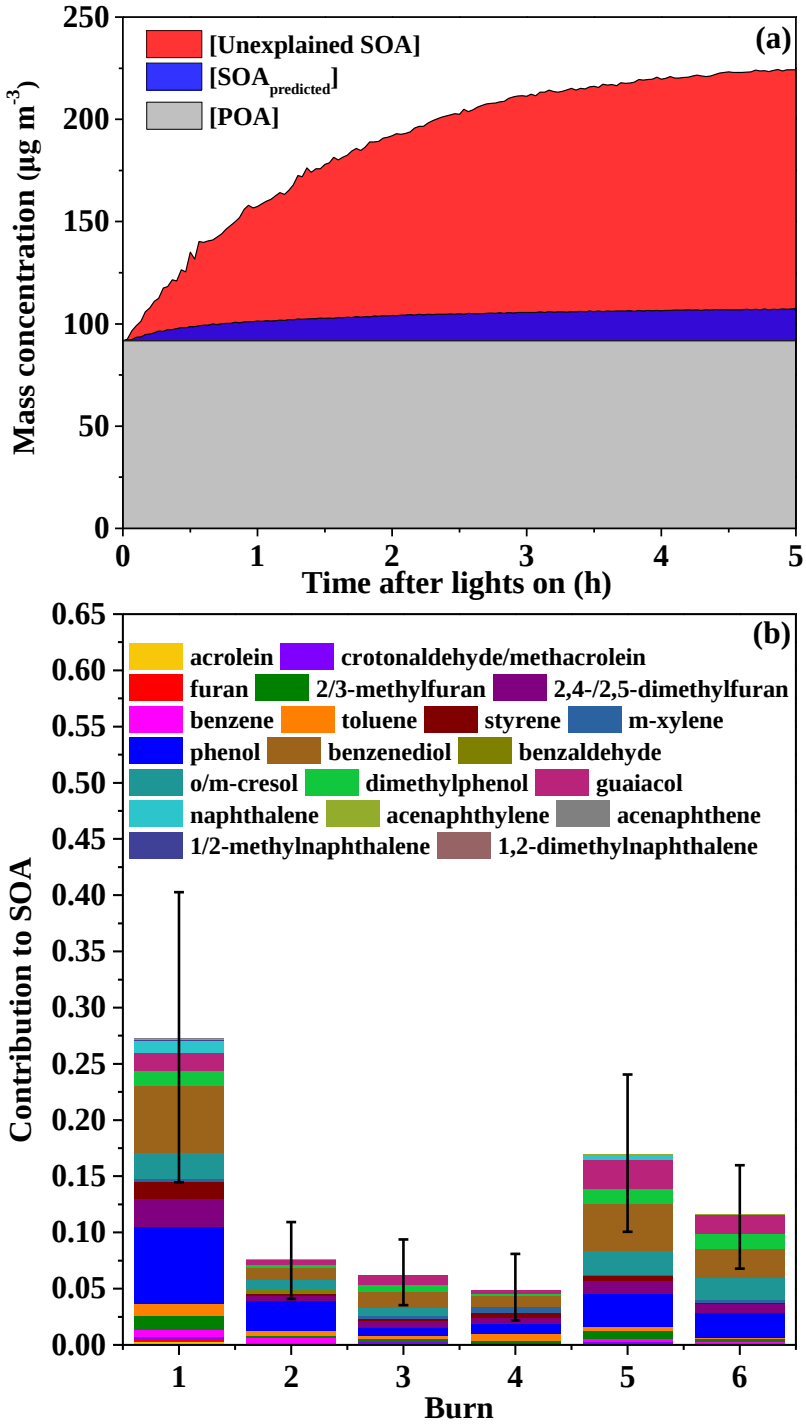

Figure 5. (a) Time series plots of concentrations of POA, secondary organic aerosol that can be explained by the reacted precursors ($SOA_{predicted}$), the difference between the formed SOA and the predicted SOA (Unexplained SOA) in Burn 6. (b) Contribution of 20 NMOGs to the formed SOA at the end of photoreactions. Error bars correspond to the range of contributions when the lowest/highest SOA yields in references were used for all precursors.

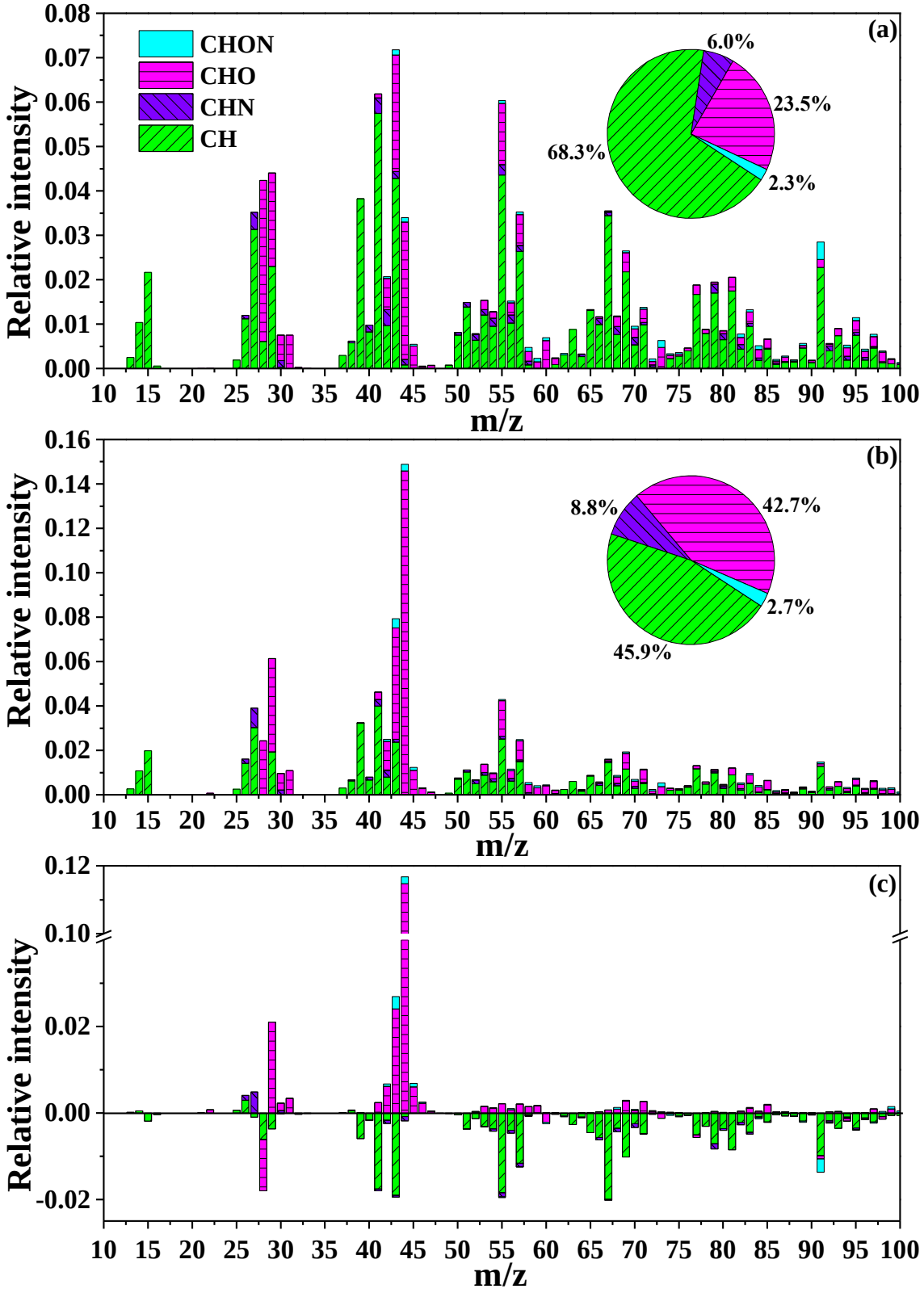

1136

1137 **Figure 6.** (a) Mass spectrum of POA; (b) mass spectrum of aged OA; (c) Difference in mass

1138 spectra between aged OA and POA. The data were all taken from Burn 5.

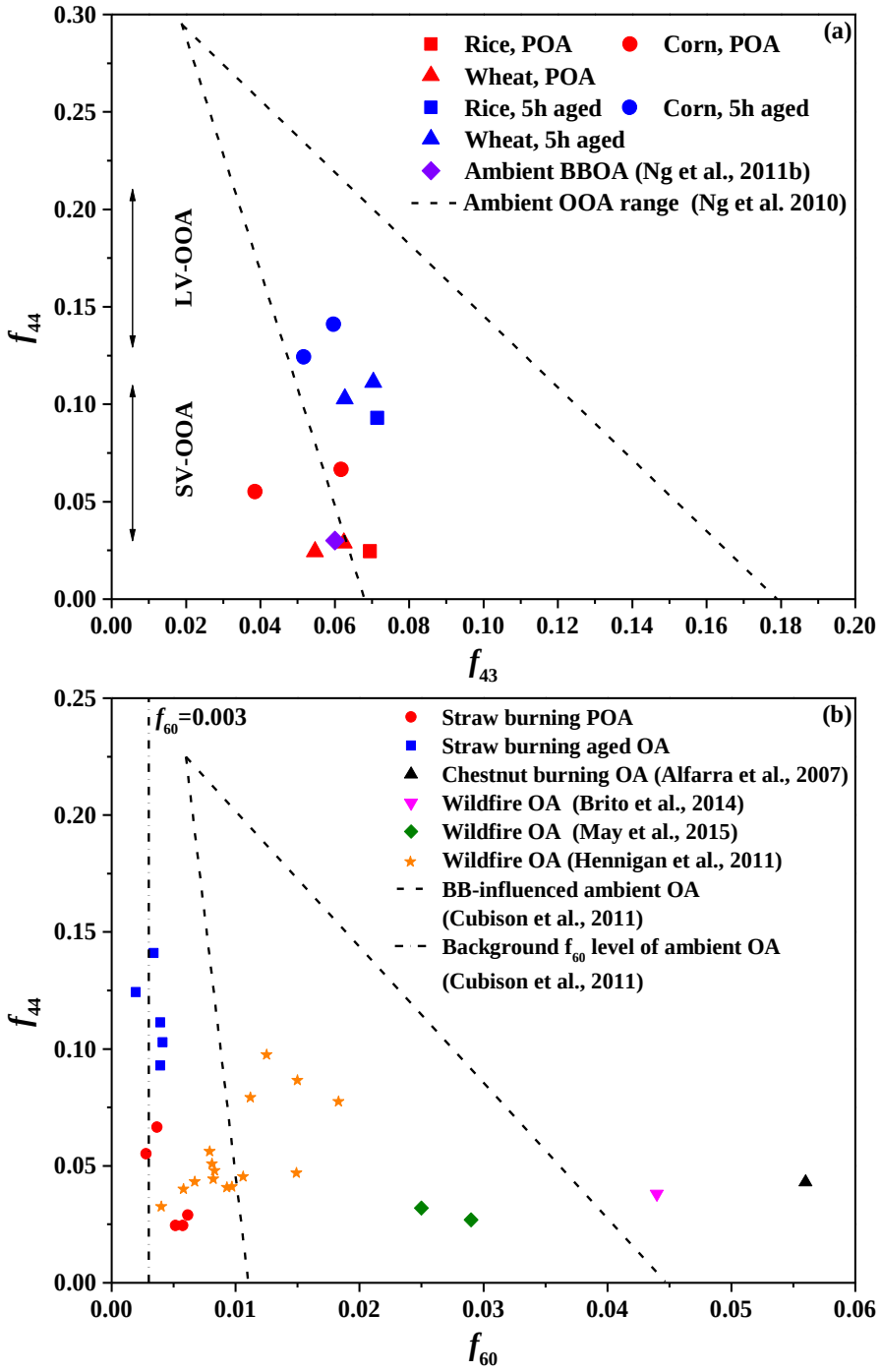

1139

1140 **Figure 7.** (a) Comparison of f_{44} vs f_{43} determined in our work with those for the ambient BBOA

1141 data sets (Ng et al., 2011b) and the ambient OOA range (Ng et al., 2010). The typical f_{44} ranges

1142 of ambient SV-OOA and LV-OOA are indicated with the vertical arrows. (b) Comparison of

1143 f_{44} vs f_{60} for straw burning OA with those for other types of biomass burning OA (Alfarra et

1144 al., 2007; Hennigan et al., 2011; Cubison et al., 2011; Brito et al., 2014; May et al., 2015).

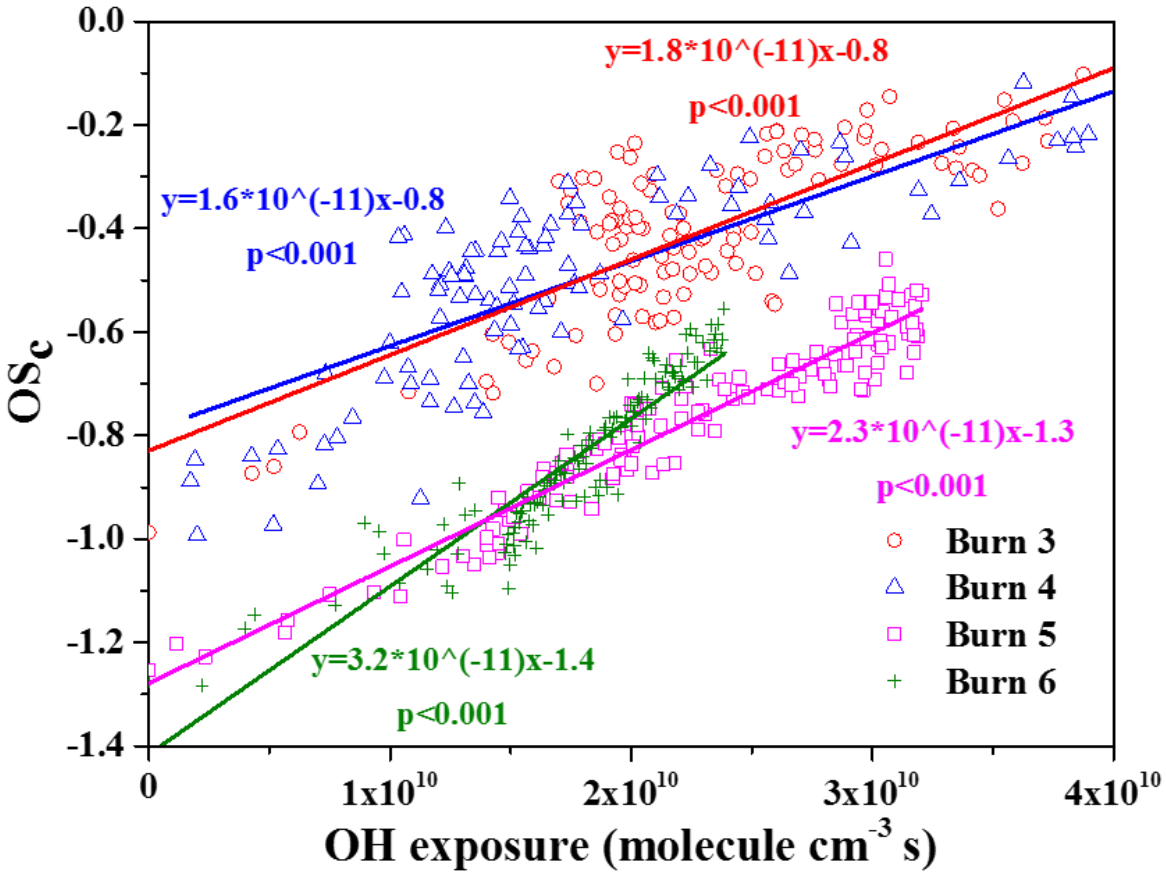

Figure 8. The growth of OA carbon oxidation state with OH exposure for burning corn (Burn 3 and 4) and wheat (Burn 5 and 6) straws. Data for burning rice straws were not included since in Burn 1 AMS was then not run in W-mode.

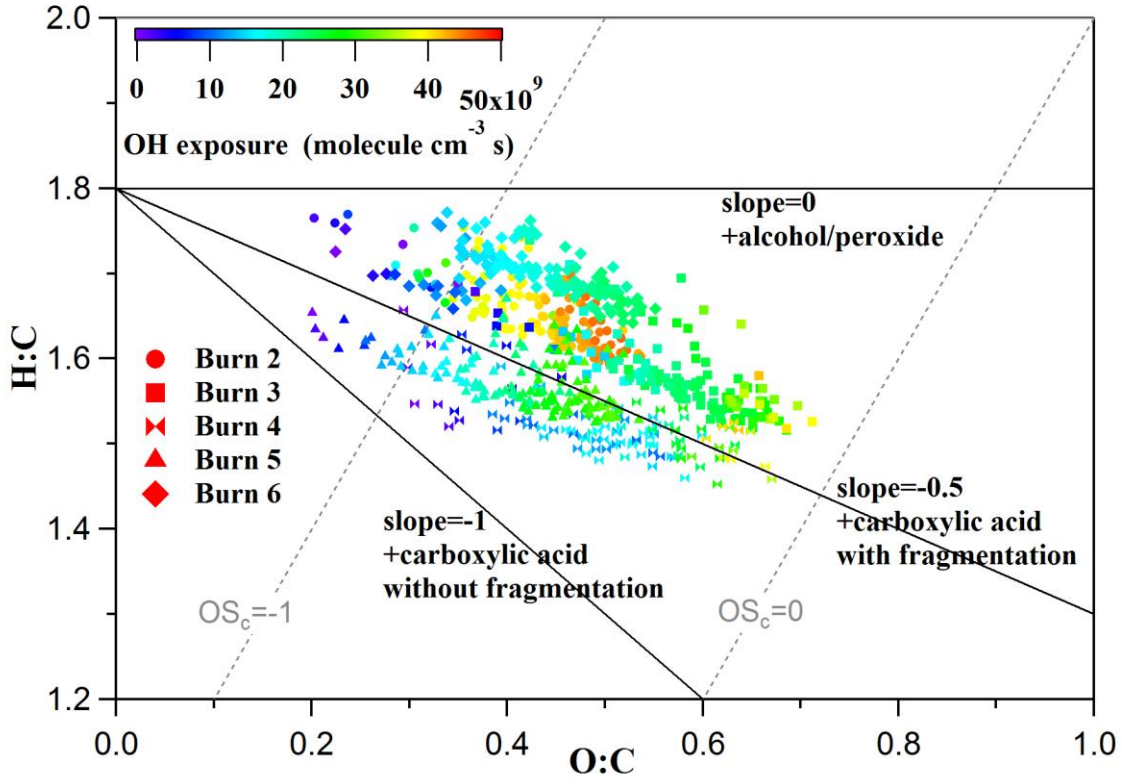

1149

1150 **Figure 9.** Van Krevelen diagram for the OA. Each slope corresponds to the addition of a

1151 specific functional group to an aliphatic carbon.